

Warm discharges in cold fresh water. Part 1. Line plumes in a uniform ambient

ANTHONY KAY

Department of Mathematical Sciences, Loughborough University,
Loughborough, Leicestershire, LE11 3TU, UK
A.Kay@Lboro.ac.uk

(Received 4 April 2006 and in revised form 25 August 2006)

Turbulent buoyant plumes in cold fresh water are analysed, assuming a quadratic dependence of density on temperature. The model is based on the assumption that entrainment velocity is proportional to vertical velocity in the plume. Numerical and asymptotic solutions are obtained for both rising and descending plumes from virtual sources with all possible combinations of buoyancy, volume and momentum fluxes. Physical sources can be identified as points on trajectories of plumes from virtual sources.

The zero-buoyancy condition, at which the plume and the ambient have equal densities but their temperatures are on opposite sides of the temperature of maximum density, is of particular importance. If an upwardly buoyant plume rising through a body of water reaches the surface before passing through its zero-buoyancy level, it will form a surface gravity current; otherwise, the plume water will return to the source as a fountain. The height at which zero buoyancy is attained generally decreases as the source momentum flux increases: greater plume velocity produces greater entrainment and hence more rapid temperature change. Descending plumes, if ejected downwards against upward buoyancy, may be classified as strongly or weakly forced according to whether they reach the zero-buoyancy condition before being brought to rest. If they do, they continue to descend with favourable buoyancy; otherwise, they may form an inverted fountain. Once a descending plume has attained downward buoyancy, it can continue to descend indefinitely, ultimately behaving like a plume in a fluid with a linear equation of state. In contrast, a rising plume will eventually come to rest, however large its initial upward buoyancy and momentum fluxes are.

1. Introduction

Power stations discharge their cooling water at temperatures approximately 10°C higher than it is taken in (Macqueen 1979). The discharged water is therefore less dense than the receiving water. With an outfall at the bed of a water body, the warm water will rise to the surface as a turbulent plume, reducing its temperature substantially as it entrains cold water from the ambient. The warm water will then spread horizontally as a surface gravity current, cooling further by entrainment and possibly by losing heat to the atmosphere: see figure 1. In this scenario, the warm water has no effect on the ecology at the bed of the water body, and there is no risk of it recirculating into a power station's intake situated at the bed.

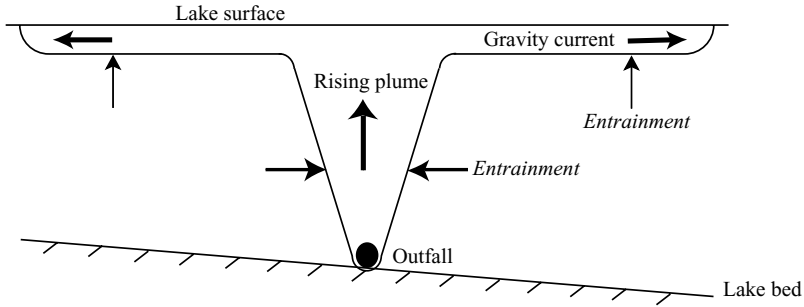


FIGURE 1. Schematic of the usual behaviour of warm water discharged from an outfall at the bed of a cooler water body.

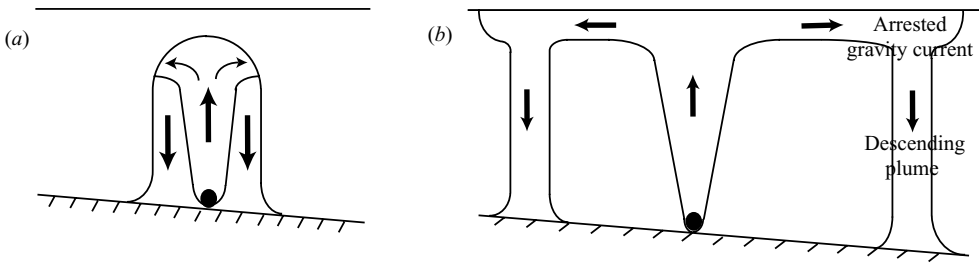


FIGURE 2. Possible behaviours of warm water discharged from an outfall at the bed of a fresh water body below the temperature of maximum density: (a) the rising plume loses buoyancy and forms a fountain; (b) the rising plume remains buoyant but the subsequent gravity current suffers buoyancy reversal, giving rise to descending plumes.

Now suppose that the receiving water is below the temperature of maximum density, approximately 4°C in fresh water but decreasing with increasing salinity in brackish water. Mixing between the warm water from the discharge and the cold receiving water can then produce water which is denser than either component, the so-called cabbelling phenomenon (e.g. Foster 1972). This may occur in the rising plume, in which case the dense water will form a fountain, returning to the bed outside the rising plume: see figure 2(a). Alternatively, the plume may reach the surface still positively buoyant, but then the warm water will inevitably become denser than the ambient water during its subsequent surface spreading: the gravity current will then be arrested, and a dense plume will descend from its head (where mixing is most intense) to the bed, as seen in the laboratory experiments of Marmoush, Smith & Hamblin (1984): see figure 2(b). In either case, water which may be as much as 8°C warmer than the ambient (in a lake at 0°C) will then spread along the bed as a dense gravity current, possibly affecting the bed ecology or entering an intake. Evidence for this was found in Lake Michigan by Hoglund & Spigarelli (1972), who measured a rise of 5.2°C from a natural ambient temperature of 0.5°C ; however, these authors were principally concerned with the biological implications of the spread of warm water along the lake bed, and did not attempt to analyse the dynamics. There, the warm water flow at the bed was considered undesirable; alternatively, if the main concern is to avoid erosion of the winter ice cover (Gu & Stefan 1993), formation of a fountain would be considered the most desirable outcome.

There are thus four possible stages of motion to be analysed: a rising plume, a surface gravity current, a descending plume, and a gravity current along the bed. The last of these has no features which are qualitatively different from situations where cabbeling does not apply. The surface gravity current will be addressed in a future paper. The remaining stages are the vertical plumes, both rising and descending, which are the object of study here. We restrict ourselves to two-dimensional geometry: thus we are modelling a line plume rising from a multiport diffuser, or descending from the head of a broad (spanwise) gravity current. The latter case includes annular descending plumes following axisymmetric spreading across the surface from above a point outfall: these may be modelled as two-dimensional if the plume's width is small compared to its radial distance from the outfall. The plumes are also assumed to be steady, as would be expected of power station cooling water discharges. Thermals arising from instantaneous releases can be modelled by a similar formalism (Turner 1973), while starting plumes, formed when the source of buoyant fluid is switched on at some initial time and then maintained, require more complicated modelling (Turner 1962); this might be relevant in understanding the plumes observed by Marmoush *et al.* (1984) descending from the head of a lock-release gravity current, but is not considered here.

We will consider only unstratified ambient conditions: in relation to protecting the bed ecology, this may be regarded as a 'worst case'. A lake which freezes over in winter will typically have inverse thermal stratification, with temperature increasing from 0°C at the surface to possibly as high as 4°C at the bed (Gu & Stefan 1993). Consider a discharge at 10°C from a lake bed, with the receiving water either (i) at a uniform temperature of 0°C , or (ii) inversely stratified. In case (i) the plume's buoyancy is lower, and its cooling rate due to entrainment is higher, than in case (ii); hence the discharge is more likely to experience buoyancy reversal before reaching the surface in our model than in a real lake. Similarly, a plume descending from the head of an arrested gravity current will have greater negative buoyancy and greater impact on the lake bed (in terms of both temperature difference and velocity) in our unstratified model than in the more realistic situation.

Whereas buoyancy reversal is the main feature of interest in rising plumes, for descending plumes a notable phenomenon is that entrainment can increase the (negative) buoyancy. Consider, for instance, a fresh water plume at 7°C , which is denser than ambient water at 0°C : as the plume descends and mixes with its surroundings, the density difference will increase until its temperature has dropped to 4°C . This is in contrast to plumes with linear mixing properties, for which entrainment always reduces the buoyancy.

The plan for the remainder of this paper is as follows. The assumptions used in modelling plume behaviour are discussed in §2. The governing equations are written down and nondimensionalized in §3, and the relation (3.20) between volume flux and momentum flux is derived as a first integral of these equations: this is a pivotal result of the paper. A thorough analysis of plume motion, based on (3.20), is presented in §4 and 5 for upward and downward motion respectively, with all possible regimes considered. In §6 we discuss the application of our results to power station cooling water discharges, which provided the motivation for this study. Some concluding remarks are given in §7. Results in §4–6 are presented graphically based on numerical integrations, but many asymptotic formulae have also been derived, which give further insight into the dynamics. However, these formulae have mainly been confined to the Appendix to avoid cluttering the main text with mathematical detail.

2. Modelling considerations

To model the behaviour of warm plumes in cold fresh water, we must account for two physical phenomena: the non-monotonic dependence of density ρ on temperature T , and the entrainment of ambient fluid. For the former, Oosthuizen & Paul (1996) state that a quadratic relationship

$$\rho = \rho_m - \beta(T - T_m)^2 \quad (2.1)$$

is a good fit to experimental data for temperatures up to 10°C, implying that (2.1) is adequate to analyse a power station cooling water discharge at 10°C into an ambient at 0°C. The constants in (2.1) are: $T_m = 3.98^\circ\text{C}$, the temperature of maximum density for fresh water at atmospheric pressure (taken as 4°C in numerical examples below); $\rho_m = 1.000 \times 10^3 \text{ kg m}^{-3}$, the density at that temperature; $\beta = 8.0 \times 10^{-3} \text{ kg m}^{-3} (\text{°C})^{-2}$ (Moore & Weiss 1973).

Entrainment will be modelled using the well-established hypothesis of Morton, Taylor & Turner (1956), that ambient fluid is entrained at a velocity proportional to the vertical velocity within the plume. A defence of this entrainment model in a case involving buoyancy reversal has been given by Caulfield & Woods (1995). An issue of particular relevance to the present application is that the plume must be fully turbulent for the entrainment assumption of Morton *et al.* (1956) to be valid. This would certainly be achieved in a power station discharge, with its large volume flux. However, in a laboratory-scale experiment, with a plume driven by the very small density differences in water close to its temperature of maximum density, the Reynolds number may be too low for the required level of turbulence. Calculations of Reynolds numbers in these situations are given in §7 below.

If the warm water reaches the surface and then spreads out horizontally, our plume model will clearly become invalid where surface impingement effects become significant. A more severe limitation applies in the case where a fountain is formed, since the entrainment will then be between the inner upflow and outer downflow, as well as from the ambient into the downflow. Bloomfield & Kerr (2000) have developed a model of fountains, taking all these interactions into account. However, the same authors' previous model assumed entrainment directly from the ambient into the upflow, with surprisingly good agreement with experimental results for the initial fountain height in the case of an axisymmetric fountain, although a greater discrepancy was found for line fountains (Bloomfield & Kerr 1998).

Whereas Bloomfield & Kerr's fountains were produced by injecting dense fluid upwards into a less dense ambient, we are considering fountains resulting from buoyancy reversal. Turner (1966) drew attention to the fundamental differences between these situations; he found that plumes with buoyancy reversal become oscillatory, and obtained scaling laws for the height, radius and period of oscillation of such plumes. Plumes and jets with buoyancy reversal have previously been considered in the context of evaporative cooling at cumulus cloud tops (Turner 1966), hydrothermal vents at the ocean floor (Turner & Campbell 1987) and volcanic plumes (Caulfield & Woods 1995), as well as fresh water below the temperature of maximum density (Gu & Stefan 1993). Of these authors, only Caulfield & Woods (1995) have provided an analysis of the plume entrainment equations with density as a quadratic function of mixing ratio. Although in their case mixing between plume and ambient fluid caused a decrease in density, their results show many similarities to those presented here, in particular when one notes our reciprocal relation (below) between volume flux and temperature (although they did not have

such a convenient parameter as temperature in terms of which to express the nonlinear density formulation). However, they only considered axisymmetric plumes and motion in one direction, and their analysis was not as detailed as that presented below.

The classical models of steady plumes use equations for conservation of mass, momentum and buoyancy (e.g. Turner 1973). Conservation of buoyancy applies if the buoyancy is a linear function of some conserved quantity (thermal energy, salinity, etc.). In the present case, the buoyancy is a nonlinear function of temperature, which is proportional to thermal energy; thus we shall use equations derived from the conservation laws for mass, momentum and thermal energy (cf. Gu & Stefan 1988; Wüest, Brooks & Imboden 1992), with the nonlinearity appearing in the buoyancy forcing term in the momentum equation. We will make the usual Boussinesq approximation, that density variations will be ignored except in the buoyancy term which is the difference between hydrostatic pressure gradients within and outside the plume. The dynamic pressure is ignored, on the basis that the plume is thin; this assumption breaks down where radial spreading due to surface impingement becomes significant.

We assume symmetry and self-similarity, so that horizontal profiles of vertical velocity $w'(x, z)$ and temperature $T'(x, z)$ (where x is the cross-plume coordinate) may be replaced by equivalent top-hat profiles, $w(z)$ and $T(z)$, both with the same half-width $b(z)$:

$$bw = \int_0^\infty w' dx, \quad (2.2)$$

$$bw^2 = \int_0^\infty w'^2 dx, \quad (2.3)$$

$$bwT = \int_0^\infty w'T' dx. \quad (2.4)$$

In case the velocity and temperature profiles are of different widths, as found by Rouse, Yih & Humphreys (1952), a transformation similar to that employed by Lee & Emmons (1961) may be used to obtain the equations in the next section.

Ambient water of uniform temperature T_∞ and density ρ_∞ is entrained into the plume at a velocity v_e , assumed to be proportional to the vertical velocity (Morton *et al.* 1956):

$$v_e = \alpha|w|. \quad (2.5)$$

The entrainment constant α has a value around 0.08 for top-hat profiles according to Turner (1973), but 0.16 according to Lee & Emmons (1961); the factor of $2/\sqrt{\pi}$ required to account for Lee & Emmons' Gaussian profile only exacerbates the discrepancy, and the later review by Turner (1986) does not provide any further information for two-dimensional plumes. Although α is scaled out of most of the calculations below, we take $\alpha = 0.1$ where a numerical value is required.

We shall consider the cases of upward and downward motion separately, orienting the vertical coordinate z and the vertical velocity w in the direction of motion in each case. Since a change in direction does not imply a switch from entrainment to detrainment, the equations describing entrainment (of mass and thermal energy) would otherwise involve a factor $|w|$, and so would in any case have to be solved separately for upward and downward motion. Furthermore, although we will see that the mathematical solution can be continued through a change in direction of the plume, this is unphysical as it represents upward- and downward-moving fluid

occupying the same space (Caulfield & Woods 1995); this is where the fountain equations of Bloomfield & Kerr (2000) would be required. We are not attempting such a complex model here, but we do expect that our analysis will provide useful information on important parameters such as maximum height of an upward plume and height at which buoyancy reversal occurs.

3. Governing equations and scalings

Conservation of mass yields, after cancelling the density (under the Boussinesq approximation), an equation for volume flux:

$$\frac{d}{dz}(bw) = \alpha w. \quad (3.1)$$

Next in the analysis of Morton *et al.* (1956) and many subsequent authors is an equation for conservation of buoyancy flux, but this depends on the buoyancy being a linear function of a conserved quantity. This is not therefore applicable in the present case, so we consider conservation of thermal energy, which yields an equation for temperature flux:

$$\frac{d}{dz}(bwT) = \alpha wT_\infty. \quad (3.2)$$

Equations (3.1) and (3.2) give the temperature in the plume:

$$T = T_\infty + \frac{F}{2bw}, \quad (3.3)$$

where F is the relative thermal flux which is conserved because of the unstratified ambient conditions:

$$F = 2bw(T - T_\infty) = \text{constant}. \quad (3.4)$$

The vertical momentum equation is

$$\frac{d}{dz}(bw^2) = \mp gb \frac{\rho - \rho_\infty}{\rho_m} \quad (3.5)$$

(Lee & Emmons 1961), where the upper and lower signs refer to upward- and downward-moving plumes respectively. Using the equation of state (2.1) to obtain the buoyancy force in terms of temperature, and then eliminating the latter by means of (3.3), this becomes

$$\frac{d}{dz}(bw^2) = \mp \frac{g\beta}{\rho_m} b (T - T_\infty)(2T_m - T - T_\infty) \quad (3.6)$$

$$= \mp \frac{g\beta}{\rho_m} \frac{F}{2w} \left(2T_m - 2T_\infty - \frac{F}{2bw} \right). \quad (3.7)$$

It will be convenient to use volume flux

$$q = bw \quad (3.8)$$

and momentum flux

$$m = bw^2 \quad (3.9)$$

(of the half-plume) as dependent variables rather than width and velocity. Noting that

$$b = \frac{q^2}{m}, \quad w = \frac{m}{q}, \quad (3.10)$$

the equations (3.1) and (3.7) for volume flux and momentum flux become

$$\frac{dq}{dz} = \frac{\alpha m}{q}, \quad (3.11)$$

$$\frac{dm}{dz} = \mp \frac{g\beta}{\rho_m} \frac{Fq}{2m} \left(2T_m - 2T_\infty - \frac{F}{2q} \right). \quad (3.12)$$

The natural scaling parameters of the problem are the temperature scale ($T_m - T_\infty$), the conserved thermal flux F and the buoyancy scale

$$g_m = \frac{g\beta(T_m - T_\infty)^2}{\rho_m}; \quad (3.13)$$

the first two of these combine to provide a volume flux scale

$$q_T = \frac{F}{T_m - T_\infty}. \quad (3.14)$$

Hence we define dimensionless variables

$$\left. \begin{aligned} Z = \left(\frac{\alpha^2 g_m}{q_T^2} \right)^{1/3} z, \quad B = \left(\frac{g_m}{\alpha q_T^2} \right)^{1/3} b, \quad W = \left(\frac{\alpha}{g_m q_T} \right)^{1/3} w, \\ Q = \frac{q}{q_T}, \quad M = \left(\frac{\alpha}{g_m q_T^4} \right)^{1/3} m, \quad \theta = \frac{T - T_\infty}{T_m - T_\infty}, \end{aligned} \right\} \quad (3.15)$$

where we are scaling out the entrainment coefficient α so that our results are independent of its numerical value. Note that a plume with $\theta = 1$ is at the temperature of maximum density, while a plume with $\theta = 2$ has the same density as the ambient, due to the equation of state (2.1): thus buoyancy reversal occurs when θ passes through the value 2.

The thermal flux equation (3.4) yields a relation between dimensionless temperature and volume flux,

$$\theta = \frac{1}{2Q}, \quad (3.16)$$

and the equations of motion (3.11) and (3.12) become

$$\frac{dQ}{dZ} = \frac{M}{Q} \quad (3.17)$$

$$\frac{dM}{dZ} = \mp \frac{4Q - 1}{4M}. \quad (3.18)$$

Eliminating Z , we obtain

$$\frac{dM}{dQ} = \mp \frac{4Q^2 - Q}{4M^2}, \quad (3.19)$$

with solution

$$M^3 = M_0^3 \mp \left(Q^3 - \frac{3}{8} Q^2 \right), \quad (3.20)$$

where M_0 is the value of M at $Q = 0$. The variation of volume flux and momentum flux with height can then be obtained by substituting from (3.20) into (3.17) and integrating numerically. It is useful to bear in mind that buoyancy forces are upward where $Q < 1/4$ and downward where $Q > 1/4$, since according to (3.16) these inequalities imply $\theta > 2$ and $\theta < 2$ respectively.

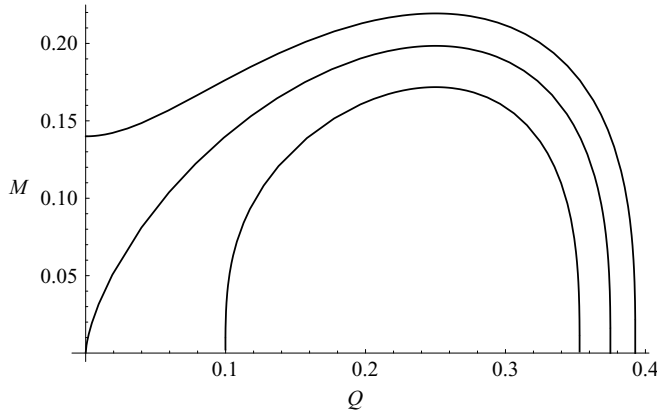


FIGURE 3. Trajectories in Q - M space from solution (3.20) for upward motion, with $M_0 = -0.14$, $M_0 = 0$ and $M_0 = 0.14$.

Plume width and velocity are obtained from dimensionless forms of (3.10). The plume's expansion angle ψ is given by

$$\tan \psi = \frac{db}{dz} = \alpha \frac{dB}{dZ} \quad (3.21)$$

$$= \alpha \left(2 - \frac{1}{W^2} \frac{dM}{dZ} \right) \quad (3.22)$$

$$= \alpha \left(1 - \frac{B}{W} \frac{dW}{dZ} \right). \quad (3.23)$$

Since α is rather small, $\tan \psi \approx \psi$ in most regions of the plumes; thus, for brevity we shall often refer to the quantity $\alpha dB/dZ$ as the expansion angle of a plume. The quantity dB/dZ will be called the *normalized expansion angle*.

The solution (3.20) is plotted for various values of M_0 , for upward motion in figure 3 and for downward motion in figure 7. Plume motion is from left to right in these plots, since the volume flux Q must always be increasing due to entrainment. Points where plume trajectories emerge from either axis represent virtual sources: on the M -axis, including the origin, the plume width is zero while its velocity and temperature are infinite; on the Q -axis, the velocity is zero but the width is infinite. The solution (3.20), in terms of the single parameter M_0 describing conditions at an unphysical virtual source, is mathematically elegant but is not so useful for providing physical insight. It is therefore useful to relate M_0 to conditions at a physical source. Plume behaviour is governed by the dimensionless temperature and Froude number at the source (Lee & Emmons 1961), defined respectively as

$$\theta_s = \frac{T_s - T_\infty}{T_m - T_\infty}, \quad \phi_s = \frac{w_s}{\sqrt{g_m b_s}}, \quad (3.24)$$

where b_s , w_s and T_s are the width, velocity and temperature at the physical source; note that we shall always define Froude numbers with respect to the constant buoyancy scale g_m rather than the buoyancy of the plume, so that the Froude number is simply a dimensionless velocity. Given positive, finite values of θ_s and ϕ_s , we can find the

corresponding coordinates in Q - M space,

$$Q_s = \frac{1}{2\theta_s}, \quad M_s = \left(\frac{\alpha\phi_s^2}{16\theta_s^4} \right)^{1/3}, \quad (3.25)$$

and substitute into (3.20) to obtain

$$M_0 = (2\theta_s)^{-4/3} \left(\alpha\phi_s^2 \pm \left(2\theta_s - \frac{3}{2}\theta_s^2 \right) \right)^{1/3}. \quad (3.26)$$

Conversely, any point (Q_s, M_s) on a trajectory in Q - M space can be regarded as a possible physical source for a plume, with

$$\theta_s = \frac{1}{2Q_s}, \quad \phi_s = \frac{M_s^{3/2}}{\alpha^{1/2}Q_s^2}. \quad (3.27)$$

4. Rising plumes

The upper, middle and lower curves in figure 3 represent a *forced plume*, a *pure plume* and a *lazy plume*, respectively, in the nomenclature preferred by Hunt & Kaye (2005). The pure plume emanates from a virtual source that supplies buoyancy flux but no momentum flux or volume flux. The forced plume is given an upward momentum flux as well as buoyancy flux at its virtual source (so may alternatively be thought of as a buoyant jet); the source has zero volume flux, and hence infinite temperature, by (3.16). In contrast, the lazy plume has less upward momentum flux than a pure plume; it comes from a virtual source with positive volume flux Q_0 , zero momentum flux and finite temperature. Its negative value of M_0 suggests a downward initial momentum flux at a source with $Q=0$ (Morton 1959), but that initial downward motion would obviously not appear in this plot, even if we make the unphysical continuation from it to the rising plume. All three plumes in figure 3 have upward momentum flux increasing to a maximum when $Q=1/4$; at this point the buoyancy force changes sign and the momentum flux then decreases to zero, so that all rising plumes eventually come to rest with infinite width and finite final volume flux Q_f (in our model, which cannot describe fountains or the oscillatory behaviour identified by Turner 1966). The value of Q_f , and also of Q_0 in the case of a lazy plume, can be found as solutions of (3.20) with $M=0$. The initial and final volume fluxes Q_0 and Q_f converge to the value $1/4$ as M_0 approaches a critical value $-2^{-7/3} \approx -0.1984$; no rising plume can exist with larger negative values of M_0 than this. The number $2^{-7/3}$ will be seen to have further significance in the context of descending plumes.

The differences between the three classes of plume are most pronounced near their respective virtual sources, as shown by the asymptotic formulae (A1)–(A12) (see Appendix, §A.1) for volume flux, momentum flux, half-width and vertical velocity close to the three classes of virtual source: note that in all cases the zero of the vertical coordinate Z is set at the virtual source. The different behaviours near the source are also apparent in figure 4, where the half-width, normalized expansion angle, velocity, temperature and momentum flux are plotted as functions of height for a pure plume and for examples of a forced plume and a lazy plume. A forced plume has an initial expansion angle of 2α as for a jet, so is broader than a pure plume for which the angle is $(4/3)\alpha$ at its source (see (A3) and (A7)); this is because the greater velocity of the forced plume in its earlier stages (figure 4c) leads to greater entrainment. In contrast, a lazy plume has infinite width at its virtual source, but the width rapidly contracts to a minimum and the velocity rises to a maximum, with minimum width occurring

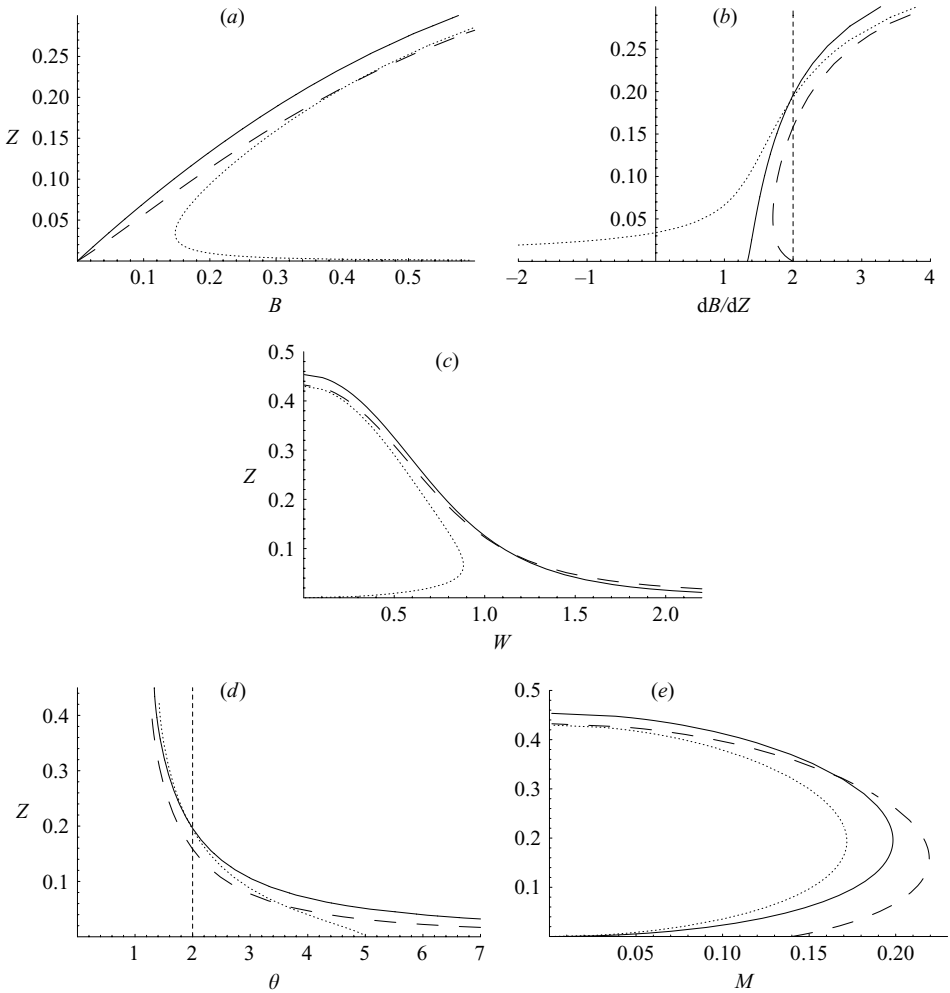


FIGURE 4. Dimensionless plume properties versus height above virtual source for a pure plume (solid curves), a forced plume with $M_0 = 0.14$ (dashed curves) and a lazy plume with $M_0 = -0.14$ (dotted curves): (a) half-width, (b) normalized expansion angle, (c) vertical velocity, (d) temperature, (e) momentum flux. The vertical line on panel (b) indicates the normalized expansion angle for a non-buoyant jet, while that on panel (d) indicates the temperature of zero buoyancy.

before maximum velocity, which in turn occurs before the point of zero buoyancy (see Appendix, § A.3). Beyond the point of maximum velocity, the lazy plume appears remarkably similar to the forced plume, while the pure plume remains the narrowest (figure 4a); but a more strongly forced plume than in the example in figure 4 would eventually become narrower than the pure plume.

The plume angle increases monotonically for the pure plume (panel b). However, the forced plume's angle initially decreases, remaining less than that for a jet while its momentum flux is increasing; it then becomes equal to the jet value of 2α at the zero-buoyancy level, and greater than the jet value when its momentum flux is decreasing: see also (3.22). As the plumes come to rest, they all spread out to infinite width (not apparent on the scale used in figure 4a).

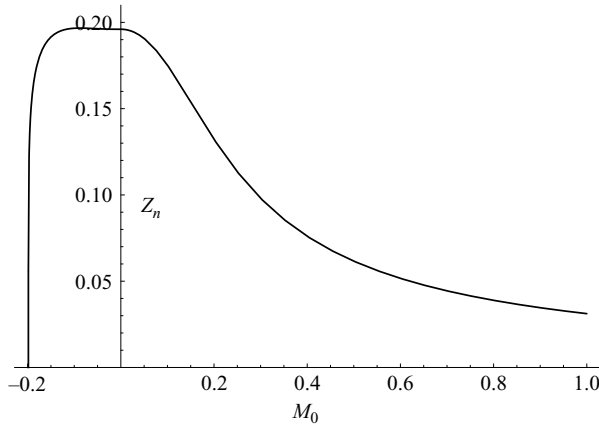


FIGURE 5. Dimensionless height of zero buoyancy, calculated from (4.1), as a function of M_0 .

The temperature plot (figure 4*d*) shows that the greater entrainment in the forced plume causes it to cool down much more rapidly than the pure plume, thus reaching the temperature of zero buoyancy at a lower level, as also shown by the positions of the maxima in momentum flux (panel *e*). The lazy plume, despite starting from a finite temperature, cools down rather slowly due to its low velocity and consequent slow entrainment, and the height at which it reaches the temperature of zero buoyancy is close to that of the pure plume. We may calculate this zero-buoyancy height as

$$Z_n = \int_{Q_0}^{1/4} \frac{Q}{M} dQ, \quad (4.1)$$

from (3.17), where we use the convention that $Q_0 = 0$ for forced and pure plumes. The height Z_n is the maximum depth of water in which a plume could reach the surface lighter than the ambient, and so spread out as a surface gravity current. It is plotted as a function of M_0 in figure 5, and asymptotic formulae valid for various ranges of M_0 are given in the Appendix, §A.2. Figure 5 clearly confirms that for forced plumes, an increase in the forcing at the source causes a decrease in the height travelled before the zero-buoyancy condition is reached (with the caveat that we are considering a virtual source here, so this may not be directly applicable to practical situations: see §6 below): for large M_0 , Z_n decreases as $1/M_0$. For lazy plumes, there is very little variation in Z_n for $-0.15 < M_0 < 0$: the maximum value of Z_n is 0.1967 at $M_0 = -0.0874$, compared with $Z_n = 0.1960$ for a pure plume. Only when M_0 comes close to the critical value $-2^{-7/3}$ does Z_n reduce significantly. A plume in this near-critical regime has a virtual source only a little above the temperature of zero buoyancy: it therefore experiences a very weak upward buoyancy force, so its velocity remains low, but the consequent slow entrainment means that it cools down very slowly and so can still travel a considerable distance before its temperature drops to $\theta = 2$.

The maximum rise height of the plume and the dimensionless temperature at that height can be found from (3.17) and (3.16) as

$$Z_f = \int_{Q_0}^{Q_f} \frac{Q}{M} dQ, \quad (4.2)$$

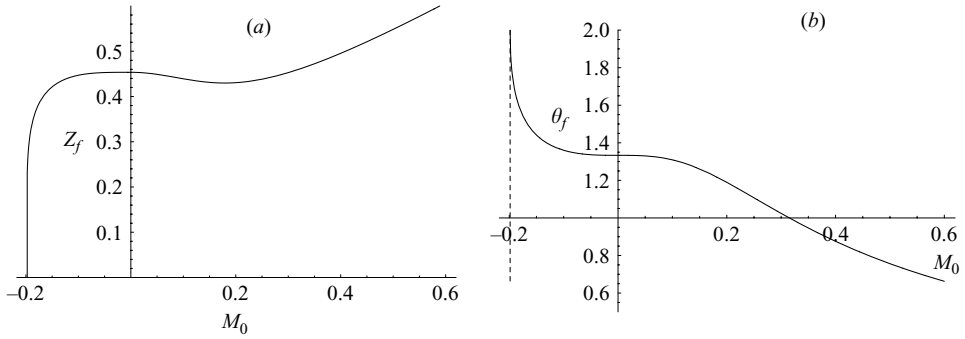


FIGURE 6. (a) Maximum rise height and (b) temperature at this height, as a function of M_0 . The vertical dashed line in (b) indicates the critical value $M_0 = -2^{-7/3}$.

$$\theta_f = \frac{1}{2Q_f} \quad (4.3)$$

and are plotted as functions of M_0 in figure 6. In our model, the plume comes to rest at the height Z_f . In reality, this will be the height of the fountain top, attained only momentarily if the oscillatory regime of Turner (1966) applies; it is also the maximum depth of water in which the plume will impinge on the surface.

The plume attains its maximum rise height when all the momentum flux attained at the point of zero buoyancy has been removed by adverse buoyancy forces. Setting $Q = 1/4$ in (3.20), the momentum flux to be removed is

$$M_n = \left(M_0^3 + \frac{1}{128} \right)^{1/3}. \quad (4.4)$$

The variation of M_n with the initial forcing M_0 is directly reflected in the amount of cooling required to bring the plume to rest (figure 6b): the fountain-top temperature θ_f varies little from its pure-plume value of $4/3$ while $|M_0| < 0.1$, but decreases as $1/M_0$ for strong forcing (when $M_n \sim M_0$) and increases rapidly towards the zero-buoyancy temperature as M_0 approaches $-2^{-7/3}$. Consequently, for moderate values of M_0 the increased entrainment is the dominant effect on Z_f as for Z_n , and we have the rather counter-intuitive result that pushing a plume harder at its source may lead to it rising less far; a similar phenomenon was found by Turner (1986) with vortex rings in a stable environment. However, this effect of entrainment is less pronounced than was found for Z_n , and Z_f reaches a minimum value of 0.4297 when $M_0 = 0.1791$, compared to $Z_f = 0.4534$ for a pure plume. For larger values of M_0 , the requirement to remove more momentum flux means that the plume can travel further, and for strong initial forcing the height of a fountain increases linearly with M_0 . For lazy plumes, the variation of Z_f with M_0 is similar to that of Z_n , except that the maximum of Z_f is at $M_0 = 0$: as laziness (negative M_0) increases from zero, the slight reduction in the amount of cooling required to bring the plume to rest cancels out the effect of reduced entrainment which caused Z_n to increase. All the above physical effects are reflected in the asymptotic formulae (see Appendix, § A.2).

5. Descending plumes

Figure 7 shows trajectories in Q - M space for downward plumes with five values of M_0 . As before, plumes with negative, zero or positive values of M_0 are described as lazy,

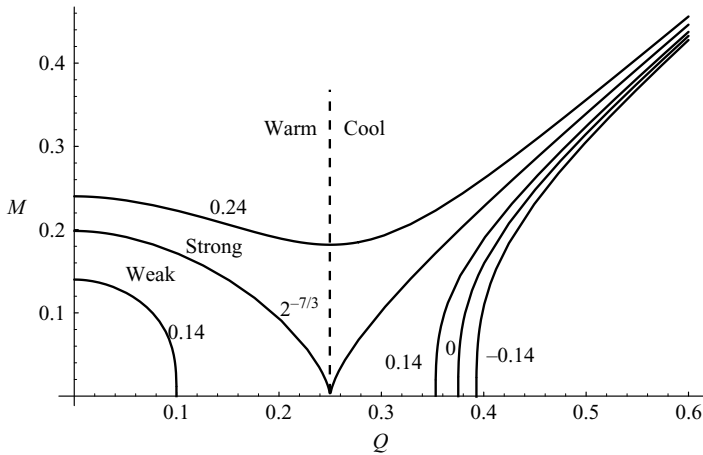


FIGURE 7. Trajectories in Q - M space from solution (3.20) for downward motion, with $M_0 = -0.14$, $M_0 = 0$, $M_0 = 0.14$, $M_0 = 2^{-7/3}$ and $M_0 = 0.24$, as identified by labels on curves. The curve for $M_0 = 2^{-7/3}$ separates strongly forced from weakly forced plumes, while the line $Q = 1/4$, corresponding to $\theta = 2$, separates the warm and cool sectors.

pure or forced, respectively; however, M_0 is now a downward momentum flux, and the forcing (or otherwise) provided by the source is with respect to downward momentum. It is clear from the figure that the important distinction among downward plumes is according to whether M_0 is greater or less than $2^{-7/3}$. The case $M_0 = 2^{-7/3}$ will be designated *critical forcing*; recall that upward plumes cannot exist with $M_0 < -2^{-7/3}$. A plume with $M_0 > 2^{-7/3}$ is described as *strongly forced*. If $0 < M_0 < 2^{-7/3}$, there are two branches of the solution: the one with $Q < 1/4$ (so that $\theta > 2$) is the *warm weakly forced* plume, while the branch with $Q > 1/4$ (so $\theta < 2$) is the *cool weakly forced* plume. Pure and lazy plumes only exist in the cool sector, because a warm ($\theta > 2$) plume has upward buoyancy and so would need downward forcing from its source in order to move downwards. It is evident from figure 7 that all plumes in the cool sector, regardless of forcing or laziness, behave similarly at large distances from the source (the *far field*), corresponding to large Q in figure 7.

The virtual source of a strongly forced plume or a warm weakly forced plume has infinite temperature, so that the buoyancy force is initially upward. The behaviour near the source is similar to that for an upward forced plume, except that the momentum flux is decreasing (as shown by the sign change in (A 2)). The plume is ejected downward, and the adverse buoyancy depletes its momentum flux; however, by entraining cold water, it is continually reducing the upward buoyancy. Weak forcing means that the initial momentum flux is insufficient to prevent the plume being brought to rest before cooling to the temperature of zero buoyancy ($\theta = 2$), whereas strong forcing means that the plume reaches this temperature with positive downward momentum and can then gain momentum flux as the buoyancy force becomes favourable (downward). A critically forced plume comes to rest exactly at the temperature of zero buoyancy, and can in principle then accelerate downwards, although this continuation may be considered unphysical as the plume has infinite width where it comes to rest; instead, we may refer separately to *warm* and *cool critically forced plumes*.

A rising lazy plume is a mathematical continuation of a descending weakly forced plume with the same value of $|M_0|$. Similarly, a descending, cool weakly forced or lazy

plume is the respective mathematical continuation of a rising, lazy or forced plume. Although it is tempting to think of a plume simply changing direction, possibly twice, this is unphysical (cf. Morton 1959): not only would it pass through a condition of infinite width, but the plume after the reversal would be passing through the same space that is occupied by the plume before the reversal. A physically realistic model for change of direction would be as a fountain, inverted in the case of a descending weakly forced plume. However, considering the mathematical connection between rising and descending plume solutions does help to clarify why rising plumes cannot exist with larger negative values of M_0 than the critical value.

We now discuss the details of plume motion for three classes of downward plume: strongly forced, warm weakly forced, and cool, with the critically forced plume considered as a limiting case of each class.

5.1. Strongly forced plumes

Figure 8 details the development of a critically forced plume (both warm and cool phases) and of strongly forced plumes with two values of M_0 , one of which is close to the critical value. The point of zero buoyancy is where the momentum flux (panel *b*) reaches its minimum and the volume flux (panel *a*) passes through the value $1/4$. For the critically forced plume, the volume flux (and hence temperature) is stationary and the vertical velocity falls to zero at this point, so that the plume is travelling a substantial distance at low velocity (hence low entrainment) under very small buoyancy forces. For strongly forced plumes, the vertical velocity (panel *e*) has a minimum beyond the point of zero buoyancy (see Appendix, §A.4). In the far field where $Q \gg M_0$, $M \sim Q$ from (3.20); (3.17) then shows that the volume flux and momentum flux both increase linearly with distance, so that the normalized expansion angle dB/dZ and the dimensionless vertical velocity W both approach unity as $Z \rightarrow \infty$ for all plumes (see Appendix, §A.5, for more details).

The variation of plume width and expansion angle (panels *c* and *d* in figure 8) may be derived from the velocity and momentum flux variations using (3.22) and (3.23). The expansion angle must change from an initial value of 2α (the angle associated with non-buoyant jets) to a final angle of α ; the latter is the angle associated with pure plumes with a linear equation of state, and occurs because the effects of the initial momentum and the nonlinear temperature-density relation are no longer felt at great distances. The expansion angle also passes through 2α at the point of zero buoyancy and through α at the point of minimum velocity. It is greater than 2α while there is an adverse buoyancy force, and less than α while the plume is accelerating; in the case of the plume with $M_0 = 0.205$, the expansion angle actually becomes negative, i.e. the plume contracts for some distance. A region of plume contraction is obviously required for the cool critically forced plume, starting from infinite width at the point of zero buoyancy, and also occurs for strongly forced plumes with $M_0 < 2^{-2/3}/3 \approx 0.2100$. On the other hand, for larger values of M_0 there is less ‘overshoot’ in the transition from the initial angle 2α to the final angle α .

The distance Z_n below the source at which zero buoyancy occurs is again given by (4.1) (with $Q_0 = 0$), and is plotted as a function of M_0 in figure 9; asymptotic formulae are given in the Appendix, §A.6. Most striking is the rapid drop in Z_n as M_0 rises a little above critical. As for rising plumes, greater velocity implies greater entrainment and hence a decrease in the distance travelled to achieve the fixed amount of cooling between the source and the zero-buoyancy condition. The low velocity and small buoyancy forces experienced by the critically forced plume around the zero-buoyancy point contrast with the much greater velocity and buoyancy forces for a plume with

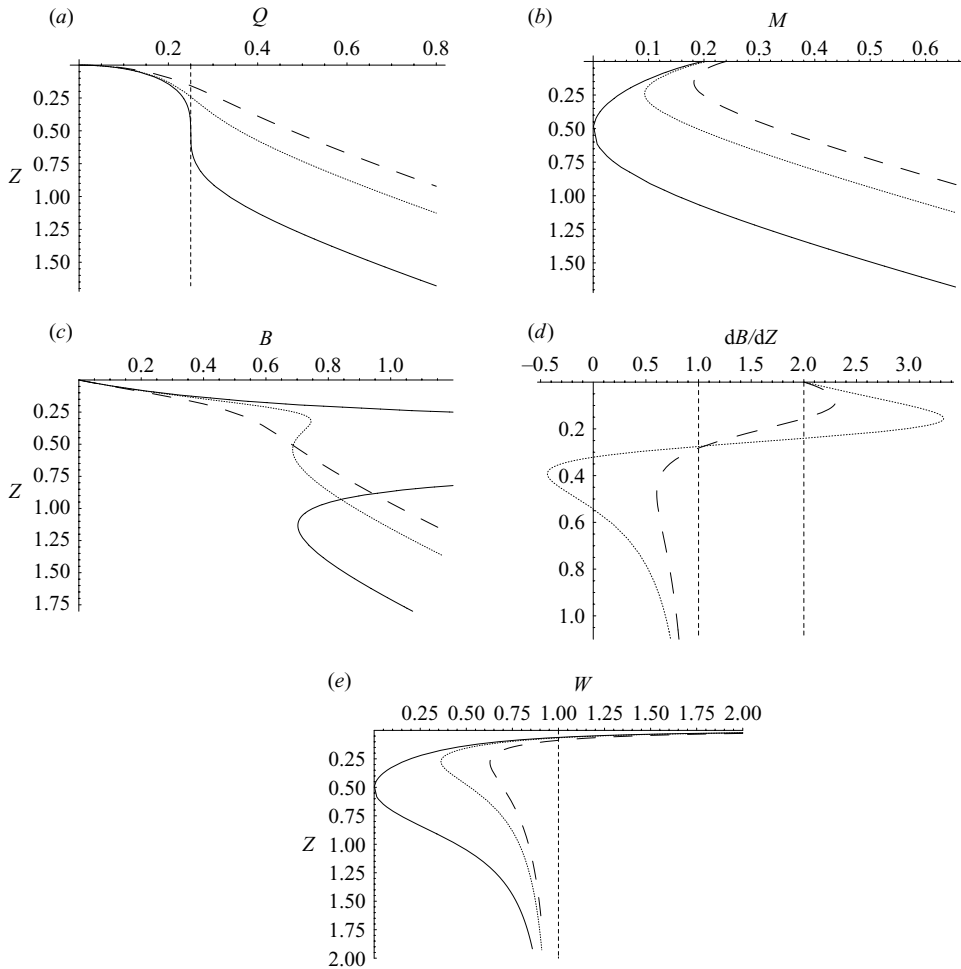


FIGURE 8. Dimensionless plume properties versus vertical distance below an infinite-temperature virtual source for a critically forced plume with $M_0 = 2^{-7/3} \approx 0.1984$ (solid curves) and strongly forced plumes with $M_0 = 0.205$ (dotted curves) and $M_0 = 0.24$ (dashed curves): (a) volume flux, (b) momentum flux, (c) half-width, (d) normalized expansion angle, (e) vertical velocity. Vertical dashed lines indicate: level of zero buoyancy in (a); normalized expansion angles for non-buoyant jets and pure plumes in (d); limiting value of velocity in far field in (e). The Z -axis is downwards to indicate orientation of plume (also in all plots below referring to descending plumes).

forcing only slightly above critical (see figure 8): hence the large difference in distances travelled.

5.2. Warm, weakly forced plumes

Figure 10 details the development of a warm critically forced plume and of warm weakly forced plumes with two values of M_0 , one of which is close to the critical value. In each case, the plume comes to rest with volume flux $Q_f \leq 1/4$ and infinite width, but the main feature of interest is the big difference made by a slight departure from critical forcing (as was the case with strongly forced plumes). A critically forced plume travels a long distance with low velocity, low entrainment and hence very gentle deceleration, but this situation is very sensitively balanced: a small decrease in

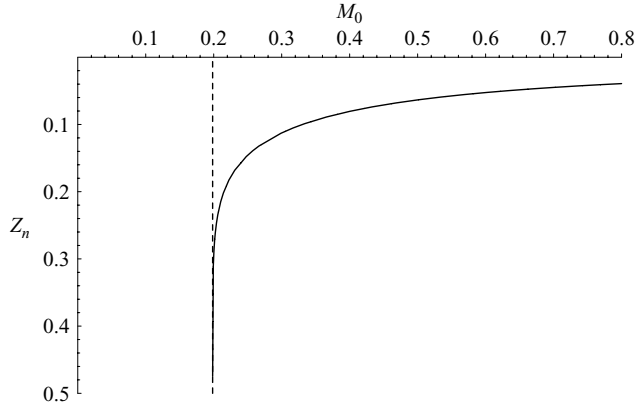


FIGURE 9. Distance downwards from source to point of zero buoyancy as a function of M_0 for strongly forced plumes. The vertical dashed line indicates the value of M_0 for a critically forced plume.

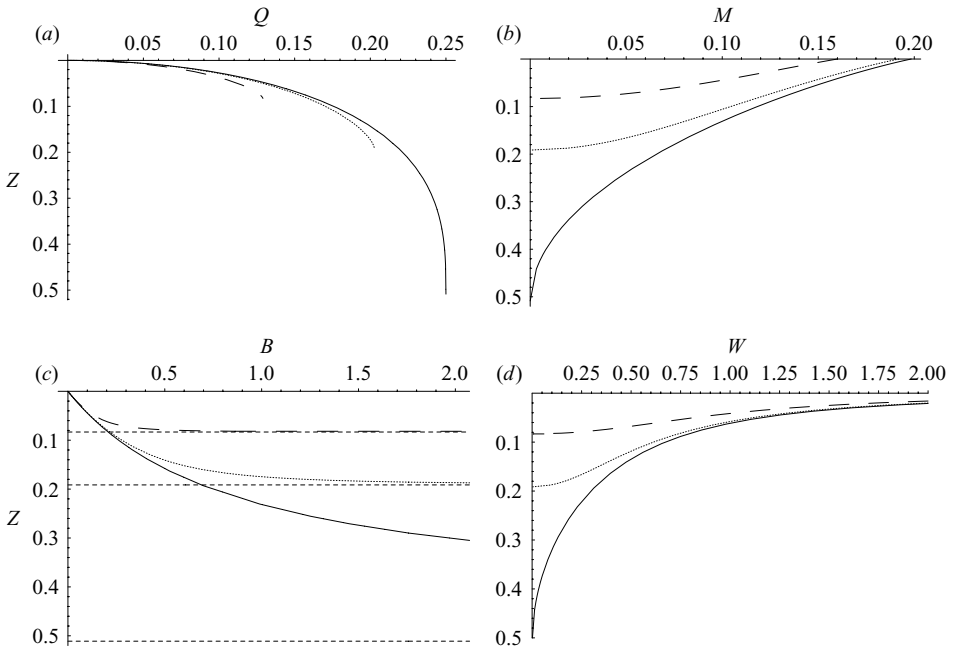


FIGURE 10. Dimensionless plume properties versus vertical distance below an infinite-temperature virtual source for a critically forced plume (solid curves) and warm weakly forced plumes with $M_0 = 0.192$ (dotted curves) and $M_0 = 0.16$ (dashed curves): (a) volume flux, (b) momentum flux, (c) half-width, (d) vertical velocity. Horizontal dashed lines in (c) indicate distances at which plumes come to rest.

initial momentum flux from the critical value $2^{-7/3} \approx 0.1984$ leads to a large reduction in total distance travelled before coming to rest. This reduction in Z_f as M_0 decreases from its critical value is characterized by the 1/6-power term in the asymptotic formula (A 56), and can be seen in figure 10(b) by comparing the Z -axis intercepts of the curves for $M_0 = 2^{-7/3}$ and $M_0 = 0.192$.

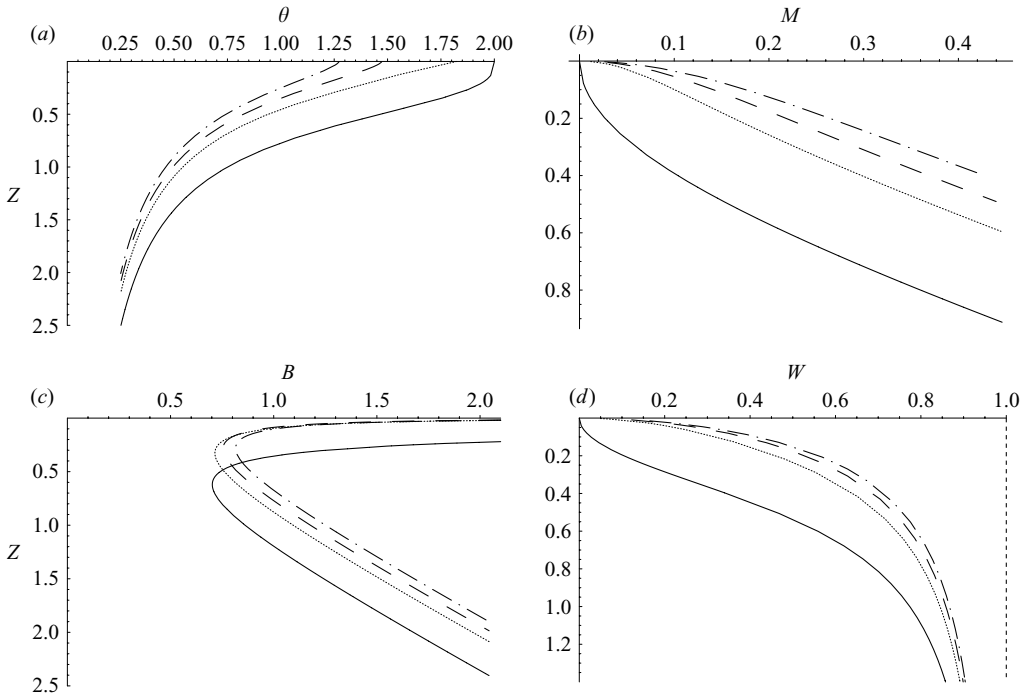


FIGURE 11. Dimensionless plume properties versus vertical distance below a finite-temperature virtual source for a cool critically forced plume (solid curves), cool weakly forced plumes with $M_0 = 0.192$ (dotted curves) and $M_0 = 0.16$ (dashed curves) and a lazy plume with $M_0 = -0.14$ (dash-dotted curves): (a) temperature, (b) momentum flux, (c) half-width, (d) vertical velocity. The vertical dashed line in panel (d) indicates the far-field limiting value of velocity.

If the initial momentum flux is small, a warm descending plume will be brought to rest rapidly by the strong adverse buoyancy force at high temperature, before it has entrained enough cold water to significantly reduce this force. Thus the distance travelled by the plume will be very small, as shown by the quadratic dependence of Z_f on M_0 in the asymptotic formula (A 55) for small M_0 . The temperature at which a warm weakly forced plume comes to rest may be calculated using (4.3), with Q_f here being identical to the Q_0 for lazy rising plumes, as given by formulae (A 20) and (A 24). This temperature decreases monotonically with increasing initial momentum flux.

5.3. Cool plumes

Here we consider plumes from virtual sources with volume flux $Q_0 \geq 1/4$, zero momentum flux and finite temperature; the value of M_0 for such a plume satisfies (3.20) with $Q = Q_0$ and $M = 0$, but cannot now be regarded as an initial momentum flux as this would require an unphysical continuation from a notional earlier stage of motion. The source of a critically forced plume is now taken as the point where it is at rest with $Q = 1/4$.

Figure 11 shows the development of a critically forced plume and three plumes with smaller values of M_0 : two of these are weakly forced, having the same values of M_0 as those in figure 10, while the third is lazy (with negative M_0); however, it is clear that there is no qualitative distinction between weakly forced and lazy plumes in this regime, whereas again the critically forced plume behaves differently from the

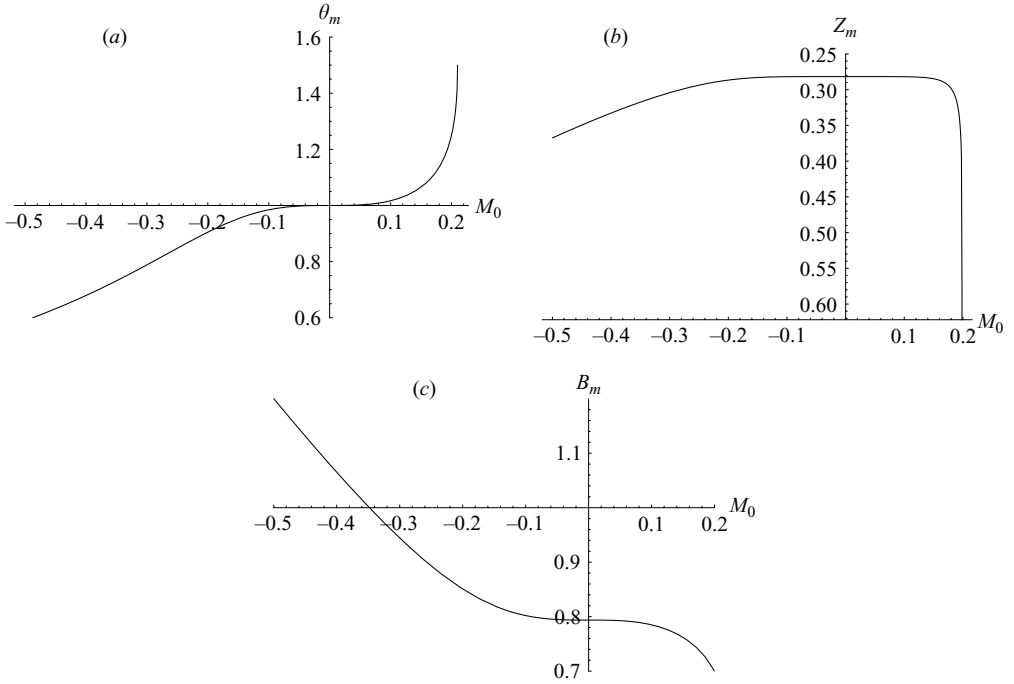


FIGURE 12. Plume properties at the neck, as a function of M_0 for cool plumes and strongly forced plumes with $M_0 < 2^{-2/3}/3$: (a) temperature, (b) distance downwards from source, and (c) half-width. The horizontal axis in (b) is drawn at the value of Z_m for a critically forced plume.

others. The distinction between the near-source behaviour of critically forced and other cool plumes is quantified in the comparison between formulae (A 9)–(A 12) and (A 13)–(A 16), and may be explained physically by the fact that there is zero buoyancy force at the critical source, whereas there is a downward force acting at any other cool source; we may suppose that the critically forced plume can move from its position of rest only due to some infinitesimal perturbation. Note that $(Q_0 - 1/4)$ has a $1/2$ power dependence on the deviation of M_0 from its critical value (from (A 22), noting the mathematical continuation from upward plumes), and this magnifies the sensitivity to slight deviations from critical forcing when forcing is quantified by the parameter M_0 . Further from the source, the contraction in width, reduction in temperature, acceleration from rest and gain in momentum flux of the critically forced plume are all delayed (as functions of distance from source) relative to other cool plumes, as shown in figure 11.

Like lazy rising plumes, cool descending plumes have infinite width at their source but are broadening at large distances from the source (see (A 51)), so the plume width must attain a minimum value at some point, known as a *neck* (Hunt & Kaye 2005). This occurs where the volume flux has the value Q_m satisfying

$$Q_m^2 - 2Q_m^3 = 4M_0^3. \quad (5.1)$$

The temperature θ_m , distance Z_m from the source and half-width

$$B_m = 2Q_m^2(Q_m^2 - 8M_0^3)^{-1/3} \quad (5.2)$$

at the neck are shown as functions of M_0 in figure 12, which also includes (except

in the Z_m plot) the small range of strongly forced plumes which have a neck. To interpret this figure it is helpful to think in terms of the temperature θ_0 at the virtual source of cool plumes: in particular, as well as $M_0 = 2^{-7/3} \approx 0.1984$ corresponding to the zero-buoyancy temperature $\theta_0 = 2$, a pure plume ($M_0 = 0$) has $\theta_0 = 4/3$ while a source at the temperature of maximum density $\theta_0 = 1$ has $M_0 = -2^{-5/3} \approx -0.3150$. One should also bear in mind that a narrow neck close to the source requires strong acceleration of the plume from the source.

Three distinct regimes are apparent in figure 12. Firstly, for $M_0 \lesssim -0.2$, i.e. source temperature close to or below the temperature of maximum density, the neck's half-width and distance from the source increase linearly with increasingly negative M_0 , while the temperature at the neck decreases. The buoyancy forces acting on the plume become weaker as the source temperature decreases below the temperature of maximum density (i.e. for larger negative M_0), and the resulting weaker acceleration of the plume produces a broader neck, further from the source. Secondly, for M_0 values above -0.2 and not too close to the critical value $2^{-7/3} \approx 0.1984$, there is very little variation in the half-width, location or temperature of the neck with M_0 . With θ_m close to the temperature of maximum density, the plume experiences fairly large buoyancy forces throughout its progress from the source to the neck, so accelerates rapidly to reach a rather narrow neck within a short distance. Finally, with M_0 close to the critical value, the initially weak buoyancy force leads to a considerable delay in reaching the neck, although this allows the plume to become even narrower than for smaller M_0 . However, the narrowest neck occurs in a strongly forced plume with $M_0 = 2^{-2/3}/3$, the greatest value of M_0 for which a neck exists. These results are quantified in the Appendix, §A.8, where precise values and asymptotic formulae for Q_m , Z_m and B_m are given.

In the far field, cool plumes behave in the same way as strongly forced plumes, as is clear from figure 7. The behaviour is detailed in the Appendix, §A.5, and the leading terms in the asymptotic formulae are of the same form as for two-dimensional plumes with a linear equation of state (Lee & Emmons 1961). Plumes in the far field have temperatures much closer to the ambient than the temperature of maximum density, so the nonlinearity of the equation of state is a small correction when considering the interaction of the plume with the ambient here. Figure 7 and equation (A 48) suggest that all plumes in the far field appear to be emanating from a finite-temperature virtual source with $Q = 1/8$, $\theta = 4$. However, in contrast to the linear case (Lee & Emmons 1961), it is not possible to locate a unique position for such an apparent source for all plumes.

6. Plumes from physical sources

While the results presented above cover all conceivable plumes in a fluid with a quadratic equation of state, they are given in terms of conditions at a virtual source and so may be difficult to interpret for studies of plumes from physical sources. There are two kinds of physical source that would appear to be of practical relevance. Firstly, a power station cooling water outfall at a lake bed would have upward buoyancy and upward vertical velocity; we consider this case in some detail below. Secondly, a plume descending from a surface gravity current that has mixed to below the temperature of zero buoyancy would have dimensionless temperature θ_s just below 2, volume flux Q_s , just above $1/4$, momentum flux M_s and Froude number ϕ_s small and positive (so that its width is finite); it would be a cool, descending plume according to the classification of Section 5. The behaviour of such a plume is described in §5.3;

the only adjustment needed to the results there is to avoid the singularity at the virtual source (see figure 11) by noting that the initial conditions prescribe a physical source position a little below the virtual source. The cool plume is the only class of descending plume which does not require its source to eject fluid downwards against the buoyancy force.

The non-dimensionalizations (3.15) may be regarded as appropriate for the power station discharge problem: the volume flux of warm water and the temperatures of both the discharge and the receiving water are fixed by power station requirements and environmental conditions, so the scales q_T and g_m are fixed. On the other hand, these non-dimensionalizations are somewhat obscure for practical purposes; in particular, with a physical source of half-width b_s it would seem natural to define dimensionless heights with respect to this parameter. We therefore define

$$\zeta \equiv \frac{z}{b_s} = \alpha^{-2/3} (2\theta_s \phi_s)^{2/3} Z, \quad (6.1)$$

where the Froude number ϕ_s and dimensionless temperature θ_s of the source are defined in (3.24). Results are presented below using both definitions of dimensionless height.

6.1. Plumes from a lake-bed outfall

We now consider a discharge at 10°C into a lake at 0°C ; given the constraint that power stations discharge their cooling water 10°C warmer than it is taken in from the ambient, this is the case of least initial buoyancy. It is therefore the worst case if one is concerned with protecting the lake bed from intrusions of warm water, but the best case if conservation of an ice cover is the principal concern.

With $T_\infty = 0^\circ\text{C}$, $T_s = 10^\circ\text{C}$ and $T_m = 4^\circ\text{C}$, the dimensionless source temperature is $\theta_s = 2.5$ and the buoyancy scale is $g_m \approx 1.3 \times 10^{-3} \text{ m s}^{-2}$. Macqueen (1979) quotes a volume flux requirement of $25 \text{ m}^3 \text{ s}^{-1}$ and a maximum discharge velocity of 2 m s^{-1} for cooling water from a power station; although he assumes a circular outfall, we shall assume that the same values would apply for a linear source of half-width b_s and length $L \gg b_s$ (so that the geometry is approximately two-dimensional). Then the source Froude number is $\phi_s \approx 22\sqrt{L}$ (where L is measured in metres), so it will be of particular interest to look at the case of large source Froude numbers.

With $\theta_s = 2.5$, the relation between the source Froude number and the parameter M_0 used in previous calculations is

$$M_0 = (0.0016\alpha\phi_s^2 - 0.007)^{1/3} \quad \text{or equivalently} \quad \phi_s = \frac{25}{\sqrt{\alpha}} \sqrt{M_0^3 + 0.007}. \quad (6.2)$$

In particular, with $\alpha = 0.1$ we find $\phi_s \approx 6.614$ when $M_0 = 0$; but the distinction between forced, pure and lazy plumes is not so significant when considering plumes from physical sources with moderate temperatures. The differences between the three classes of plume are most pronounced near a virtual source, and figure 4 shows that they all develop in rather similar ways from a source with $\theta_s = 2.5$. However, it is of interest to find the height of zero buoyancy and maximum fountain height for plumes from such a source: these heights are plotted as functions of source Froude number (which is within the outfall designer's control) in figures 13 and 14. Note that $\phi_s = 0$ corresponds to $M_0 \approx -0.1913$ while $\phi_s = 50$ corresponds to $M_0 \approx 0.7325$.

For fixed volume flux and temperature at the source, the height of zero buoyancy Z_{ns} (where the subscript s indicates a height measured from a physical source) decreases monotonically with increasing Froude number. This is similar to the behaviour of Z_n

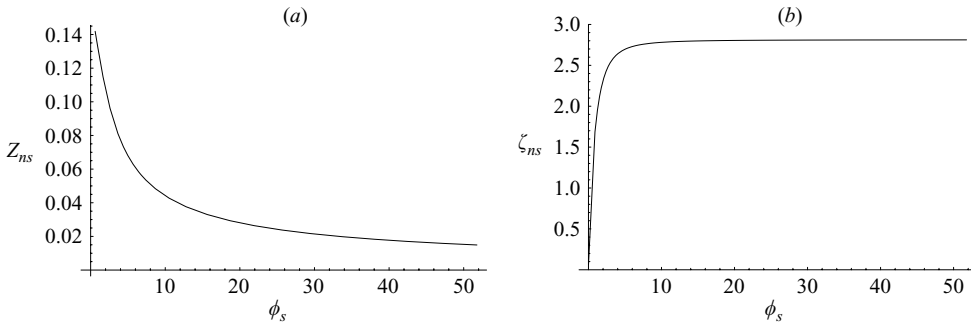


FIGURE 13. Height of zero buoyancy as a function of source Froude number for a source with dimensionless temperature $\theta_s = 2.5$, assuming $\alpha = 0.1$. Dimensionless heights defined by (a) (3.15) and (b) (6.1).

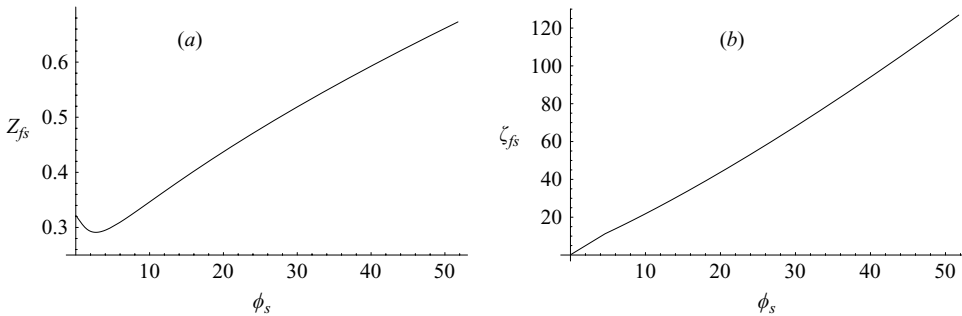


FIGURE 14. Maximum fountain height as a function of source Froude number for a source with dimensionless temperature $\theta_s = 2.5$, assuming $\alpha = 0.1$. Dimensionless heights defined by (a) (3.15) and (b) (6.1).

(measured from a virtual source) for positive M_0 (see figure 5): indeed, for large M_0 , the leading-order term in the expansion (A 31) for Z_n should simply be multiplied by $(1 - 4/\theta_s^2) = 0.36$ for $\theta_s = 2.5$, to obtain the asymptotic behaviour of Z_{ns} . In terms of source Froude number, we obtain

$$Z_{ns} \sim 2^{-11/3} \left(1 - \frac{4}{\theta_s^2}\right) \theta_s^{4/3} \alpha^{-1/3} \phi_s^{-2/3} + O(\phi_s^{-8/3}) \tag{6.3}$$

as $\phi_s \rightarrow \infty$. The discrepancy between the behaviour of Z_{ns} and the non-monotonicity of Z_n when M_0 is negative is because the temperature of the virtual source is not fixed as M_0 varies in this range, whereas θ_s is fixed.

For fixed outfall width, figure 13(b) shows the height of zero buoyancy increasing monotonically with Froude number, with

$$\zeta_{ns} \rightarrow \frac{1}{8\alpha} (\theta_s^2 - 4) \quad \text{as } \phi_s \rightarrow \infty; \tag{6.4}$$

this limiting value of ζ_{ns} is 2.8125 when $\theta_s = 2.5$ and $\alpha = 0.1$. The maximum water depth in which a line discharge at 10°C can spread across the surface of a lake at 0°C is less than three times the outfall width, irrespective of exit velocity; for a fixed volume flux requirement, the possibility of surface spreading is maximized by making the outfall as wide as possible, keeping Froude number low as indicated in figure 13(a).

For fixed volume flux, the maximum fountain height is a non-monotonic function of source Froude number, but the minimum in figure 14(a) is not directly comparable with that in figure 6(b) which occurs at a different value of ϕ_s : the elevation of the physical source above its corresponding virtual source does not vary in a similar way to the fountain height. However, the underlying reason is the same: for small ϕ_s the dominant effect is that entrainment increases with Froude number so that the plume loses buoyancy faster, but for larger ϕ_s the requirement to remove more momentum means that the plume can travel further. For large ϕ_s , the distance from the virtual source to the fountain top ($Z_f = O(\phi_s^{2/3})$ from (A 33)) is much larger than that between the virtual and physical sources, which is of the same order as the zero-buoyancy height ($Z_{ns} = O(\phi_s^{-2/3})$); thus, to leading order, $Z_{fs} \sim Z_f$ in the limit as $\phi_s \rightarrow \infty$. With fixed outfall width, the asymptotic dependence of fountain height on source Froude number is

$$\zeta_{fs} \sim \frac{C_1}{2} \alpha^{-1/3} \theta_s^{-2/3} \phi_s^{4/3} + \frac{2^{2/3} \pi}{12\sqrt{3}} \alpha^{-2/3} \theta_s^{2/3} \phi_s^{2/3} + \alpha^{-1} \left(\frac{3}{32} \theta_s^2 - \frac{1}{2} \right) + O(\phi_s^{-2/3}) \quad (6.5)$$

(obtained from (A 33) with C_1 defined in (A 17)); the distance between virtual and physical sources is accounted for in the constant term. Comparing figures 14 and 13, the top of the fountain is more than 40 times the zero-buoyancy height for $\phi_s = 50$. Thus, an outfall with a high Froude number (high exit velocity from a narrow orifice) gives the worst of both worlds: the warm water will return to the lake bed as a fountain unless the water is very shallow, but the fountain will affect the surface ice cover unless the water is very deep.

7. Conclusions

More sophisticated models of turbulent plumes, taking account of a nonlinear equation of state as well as a variety of other factors, have been presented elsewhere, e.g. Wüest *et al.* (1992). However, with such models a new numerical solution is required for each specific application. The present study is concerned solely with the effects of a quadratic equation of state; this focus has allowed us to make a thorough study, obtaining asymptotic as well as numerical solutions for all possible regimes. Plumes are considered to originate in virtual sources, allowing any physical source to be interpreted as a point on such a plume's trajectory. The classification into forced, pure and lazy plumes, used by Hunt & Kaye (2005) but having its origin in the work of Morton (1959), has needed to be refined: plumes that are forced to descend against upward buoyancy may be strongly, critically or weakly forced.

The study was motivated by the temperature–density relationship of fresh water below 10°C, but the results could be adapted to other fluids with a quadratic dependence of density on mixing ratio, e.g. volcanic plumes (Caulfield & Woods 1995) or certain chemical mixtures (Turner 1966). In these other applications, it is possible that physical sources other than those considered in §6 above may be realistic.

For rising plumes, the most important parameters to be calculated are the zero-buoyancy height and the fountain-top height. If the receiving water depth is less than the zero-buoyancy height, the warm water will travel some distance from the discharge site as a surface gravity current; otherwise, it will form a fountain, returning to the bed close to the outfall from which it is discharged. We have shown that the zero-buoyancy height may be rather small: less than 3 times the outfall width for a discharge at 10°C into receiving water at 0°C. Although the zero-buoyancy height

would increase as the ambient temperature approaches the temperature of maximum density (for a fixed 10°C temperature difference between a power station discharge and the ambient), this does indicate that it may be difficult to avoid the lake bed close to an outfall being affected by the return of warm water, as observed by Høglund & Spigarelli (1972). Even where a surface gravity current does form, it will eventually lose buoyancy so that warm water will return to the lake bed, albeit cooled more by mixing than in a fountain and removed some distance from the outfall.

For fixed volume flux, the zero-buoyancy height decreases with increasing source Froude number ϕ_s . This is due to the increased entrainment, and hence faster drop in temperature, when the velocity is greater: it is counter-productive to give the discharge a push at the outfall. For small source Froude numbers, the same effect applies to the fountain-top height, which is the minimum depth of water in which a rising plume would impinge on the surface; however, for moderate and large source Froude numbers, this height increases with ϕ_s . Fountain-top height is of importance if one is concerned about erosion of an ice cover. Thus, keeping the source Froude number low is advisable whether one is concerned with minimizing impact on the lake bed or on the surface.

In a Boussinesq fluid with a linear equation of state, changing the sign of the initial buoyancy and momentum fluxes is simply equivalent to inverting gravity. This is not true with our quadratic equation of state. In sufficiently deep water, a rising plume will eventually come to rest however large the initial upward buoyancy and momentum fluxes are, whereas a descending plume with downward buoyancy will continue to descend indefinitely. Far from its source, a descending plume will behave like a plume in a linear fluid with the same thermal expansion (or contraction) coefficient as the quadratic fluid at its ambient temperature. Of more interest is the fact that entrainment will increase the buoyancy of a plume between the temperatures of zero buoyancy and maximum density, whereas in a linear fluid entrainment always results in a decrease of buoyancy.

Some caution needs to be exercised in using the present results to predict the behaviour of real plumes, especially if laboratory experiments are used either to test the theory or to model larger-scale flows in the environment. Our governing equations assume self-similarity and the entrainment model of Morton *et al.* (1956), and we now consider two restrictions on the validity of these assumptions. Firstly, they only become valid at a distance of several outfall widths from the plume source. Our predictions of zero-buoyancy height for a discharge at 10°C into an ambient at 0°C fall within the near-source region where our equations may not be accurate; nevertheless, we do expect our predictions to be qualitatively correct. Secondly, the entrainment model requires the plume to be fully turbulent, a condition usually obtained with a Reynolds number $Re > 2000$ according to Fischer *et al.* (1979). This criterion will be comfortably exceeded in a power station discharge; for instance, with an outfall of width only 10 cm and a discharge velocity of 2 m s^{-1} , $Re \approx 1.5 \times 10^5$, given a kinematic viscosity $\nu \approx 1.3 \times 10^{-6}\text{ m}^2\text{ s}^{-1}$ for water at 10°C (Batchelor 1967). However, consider a rising plume at 10°C issuing from an orifice of width $b_s = 1\text{ cm}$ (fairly typical of laboratory experiments) into an ambient at 0°C : if we specify a pure plume, for which the source Froude number is $\phi_s \approx 6.6$ (from (6.2)), the exit velocity is $w_s \approx 0.024\text{ m s}^{-1}$, so $Re < 200$ at the source. Even at the maximum rise height, the volume flux will be less than twice its value at the source ($Q_s = 0.2$ for $\theta_s = 2.5$, and $Q_f = 0.375$ for a pure plume), so the Reynolds number (proportional to Q) will be below 400 throughout the plume. This is insufficient for self-generated turbulence;

such an experiment would be of considerable interest in itself, but the results would not then be representative of larger-scale flows in the fresh water environment. An alternative approach in the laboratory would be to generate turbulence artificially, e.g. using crosshairs (Bloomfield & Kerr 1998).

Possible directions for further theoretical research would include axisymmetric geometry and the effects of ambient stratification. It will also be important to model the entrainment in a fountain properly, as was done by Bloomfield & Kerr (2000), and the oscillatory behaviour noted by Turner (1966) should be investigated further.

This paper was improved following useful comments by referees on an earlier version.

Appendix. Asymptotic formulae, their relation to physical effects, and other mathematical details

A.1 Rising plumes: behaviour near virtual source

We distinguish four classes of virtual source. Note that where \pm or \mp signs are used, the upper and lower signs apply to rising and descending plumes, respectively. The formulae below all apply in the limit as $Z \rightarrow 0$.

(a) *Infinite-temperature sources.* These sources have zero volume flux and positive momentum flux M_0 . Apart from cool, weakly forced, descending plumes (see (c) below), all forced plumes, whether rising or descending, emanate from an infinite-temperature source:

$$Q \sim (2M_0)^{1/2} Z^{1/2} + O(Z^{3/2}), \quad (\text{A } 1)$$

$$M \sim M_0 \left(1 \pm \frac{1}{4M_0^2} Z + O(Z^{3/2}) \right), \quad (\text{A } 2)$$

$$B \sim 2Z + O(Z^2), \quad (\text{A } 3)$$

$$W \sim \left(\frac{M_0}{2} \right)^{1/2} Z^{-1/2} + O(Z^{1/2}). \quad (\text{A } 4)$$

(b) *Pure sources.* These have zero volume flux and zero momentum flux. They are sources for rising pure plumes.

$$Q \sim \left(\frac{8}{9} \right)^{1/4} Z^{3/4} + O(Z^{3/2}), \quad (\text{A } 5)$$

$$M \sim \left(\frac{Z}{2} \right)^{1/2} + O(Z^{5/4}), \quad (\text{A } 6)$$

$$B \sim \frac{4}{3} Z + O(Z^{7/4}), \quad (\text{A } 7)$$

$$W \sim \left(\frac{9}{32} \right)^{1/4} Z^{-1/4} + O(Z^{1/2}). \quad (\text{A } 8)$$

(c) *Finite-temperature sources.* These have positive volume flux Q_0 and zero momentum flux. Lazy rising plumes and cool descending plumes (except for case

(d) below) emanate from finite-temperature sources:

$$Q \sim Q_0 + \frac{\sqrt{2}}{3} \frac{|1 - 4Q_0|^{1/2}}{Q_0} Z^{3/2} + O(Z^3), \quad (\text{A } 9)$$

$$M \sim \left| \frac{1 - 4Q_0}{2} \right|^{1/2} Z^{1/2} + O(Z^2), \quad (\text{A } 10)$$

$$B \sim \left| \frac{2}{1 - 4Q_0} \right|^{1/2} Q_0^2 Z^{-1/2} + O(Z), \quad (\text{A } 11)$$

$$W \sim \left| \frac{1 - 4Q_0}{2} \right|^{1/2} \frac{1}{Q_0} Z^{1/2} + O(Z^2). \quad (\text{A } 12)$$

(d) *Critical sources.* The formulae (A 9)–(A 12) are singular in the limit $Q_0 \rightarrow 1/4$. A source with volume flux $Q_0 = 1/4$ and zero momentum flux gives rise to a cool, critically forced, descending plume:

$$Q \sim \frac{1}{4} + \frac{8}{9} Z^3 + O(Z^6), \quad (\text{A } 13)$$

$$M \sim \frac{2}{3} Z^2 + O(Z^5), \quad (\text{A } 14)$$

$$B \sim \frac{3}{32} Z^{-2} + O(Z), \quad (\text{A } 15)$$

$$W \sim \frac{8}{3} Z^2 + O(Z^5). \quad (\text{A } 16)$$

A.2 Rising plumes: height of zero buoyancy and height of plume top

We present asymptotic formulae for Z_n and Z_f valid in four ranges of M_0 , which together account for all the variation of these heights shown in figures 5 and 6(a). The formulae are derived from the integrals (4.1) and (4.2), using the method described in § 3.4 of Hinch (1991) to account for a global contribution in addition to local contributions from one or both ends of the range of integration. There is an added complication that the limits of integration Q_0 (for lazy plumes) and Q_f are given as asymptotic expansions in M_0 (also presented below), so that the asymptotic analysis requires a further rescaling each time the expansion for Z_n or Z_f is evaluated to the order of the next term in the expansion of Q_0 or Q_f . Expansions for the plume-top temperature θ_f can be derived from those for Q_f by means of the relation (3.16). All our expansions, including the order of the first neglected terms, have been checked by comparison with numerical integrations.

For neatness, we use the symbols C_1 , C_2 for the following numerical constants which appear frequently:

$$C_1 = \frac{\Gamma(\frac{5}{6})\Gamma(\frac{2}{3})}{\sqrt{\pi}} \approx 0.8624, \quad (\text{A } 17)$$

$$C_2 = 2^{-1/3} \int_0^{2/3} t^{-2/3}(1-t)^{-1/3} dt \approx 2.2446. \quad (\text{A } 18)$$

(a) M_0 close to critical. The critical value of M_0 is $-2^{-7/3}$ so the expansions are in terms of the deviation from this value,

$$M_d \equiv M_0 + 2^{-7/3}. \quad (\text{A } 19)$$

As $M_0 \searrow -2^{-7/3}$:

$$Q_0 \sim \frac{1}{4} - 2^{-5/6} M_d^{1/2} - \frac{2^{1/3}}{3} M_d + \frac{2^{5/2}}{9} M_d^{3/2} + O(M_d^2), \quad (\text{A } 20)$$

$$Z_n \sim 2^{-41/18} 3^{2/3} \left\{ C_1 M_d^{1/6} - \frac{2^{1/6}}{3} M_d^{2/3} - \frac{2^{7/3} 5 C_1}{21} M_d^{7/6} + O(M_d^{5/3}) \right\}, \quad (\text{A } 21)$$

$$Q_f \sim \frac{1}{4} + 2^{-5/6} M_d^{1/2} - \frac{2^{1/3}}{3} M_d - \frac{2^{5/2}}{9} M_d^{3/2} + O(M_d^2), \quad (\text{A } 22)$$

$$Z_f \sim 2^{-41/18} 3^{2/3} \left\{ 2C_1 M_d^{1/6} - \frac{2^{10/3} 5 C_1}{21} M_d^{7/6} + O(M_d^{13/6}) \right\}. \quad (\text{A } 23)$$

The leading-order $1/6$ powers of M_d give the rapid rise in Z_n and Z_f as M_0 increases from the critical value, as seen in figures 5 and 6. At leading order, the distance travelled by the plume while gaining momentum is equal to that travelled while losing momentum (i.e. $Z_f \sim 2Z_n$), but this symmetry is broken at $O(M_d^{2/3})$.

(b) *Small negative M_0 .* As $M_0 \nearrow 0$:

$$Q_0 \sim \frac{2^{3/2}}{3^{1/2}} |M_0|^{3/2} + \frac{32}{9} |M_0|^3 + \frac{2^{15/2} 5}{3^{7/2}} |M_0|^{9/2} + O(|M_0|^6), \quad (\text{A } 24)$$

$$Z_n \sim 2^{-8/3} (C_2 - 1) + \frac{2^{13/3}}{3} |M_0|^3 - \frac{2^{13/2} 3^{1/2} C_1}{7} |M_0|^{7/2} + O(|M_0|^6), \quad (\text{A } 25)$$

$$Q_f \sim \frac{3}{8} - \frac{64}{9} |M_0|^3 - \frac{2^{16}}{3^5} |M_0|^6 + O(|M_0|^9), \quad (\text{A } 26)$$

$$Z_f \sim \frac{\pi}{4\sqrt{3}} - \frac{2^{13/2} 3^{1/2} C_1}{7} |M_0|^{7/2} + O(|M_0|^{13/2}). \quad (\text{A } 27)$$

The values of Z_n and Z_f for a pure plume ($M_0=0$) are given by the leading-order (constant) terms in the expansions (A 25) and (A 27). The terms of order $|M_0|^{7/2}$ (and also $O(|M_0|^{n+7/2})$, ($n=1, 2, \dots$)) are local contributions from a region where $Q = O(|M_0|^{3/2})$ at the start of the integration range in (4.1) and (4.2); i.e. they represent the effect of the (small) initial momentum flux deficit (relative to a pure plume), which is felt in a region close to the virtual source. The terms of order $|M_0|^{3n}$ ($n=1, 2, \dots$) in (A 25) are global contributions, representing the effect of decreased entrainment allowing the plume to travel further before reaching the condition of zero buoyancy; they are exactly cancelled out in (A 27), as the amount of further entrainment required to bring a plume to rest after reaching the zero-buoyancy level is less for a lazier plume.

The coincidence of opposing terms of high but close orders ($|M_0|^3$ and $|M_0|^{7/2}$) in (A 25) gives the behaviour seen in figure 5 and more clearly in figure 15, where the maximum value of Z_n occurs at a moderate negative value of M_0 , but is barely above the value of Z_n for a pure plume.

(c) *Small positive M_0 .* As $M_0 \searrow 0$:

$$Z_n \sim 2^{-8/3} (C_2 - 1) - 2M_0^2 - \frac{2^{13/3}}{3} M_0^3 + \frac{2^{11/2} 3 C_1}{7} M_0^{7/2} + O(M_0^5), \quad (\text{A } 28)$$

$$Q_f \sim \frac{3}{8} + \frac{64}{9} M_0^3 - \frac{2^{16}}{3^5} M_0^6 + O(M_0^9), \quad (\text{A } 29)$$

$$Z_f \sim \frac{\pi}{4\sqrt{3}} - 2M_0^2 + \frac{2^{11/2} 3 C_1}{7} M_0^{7/2} + O(M_0^5) \quad (\text{A } 30)$$

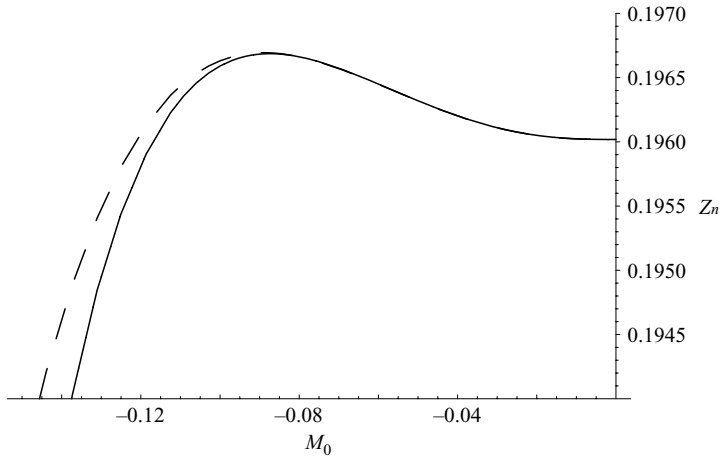


FIGURE 15. Dimensionless height of zero buoyancy, as a function of M_0 for small and moderate negative values of M_0 . Solid line: numerical integration of (4.1); dashed line: asymptotic formula (A 25) up to $O(|M_0|^{7/2})$.

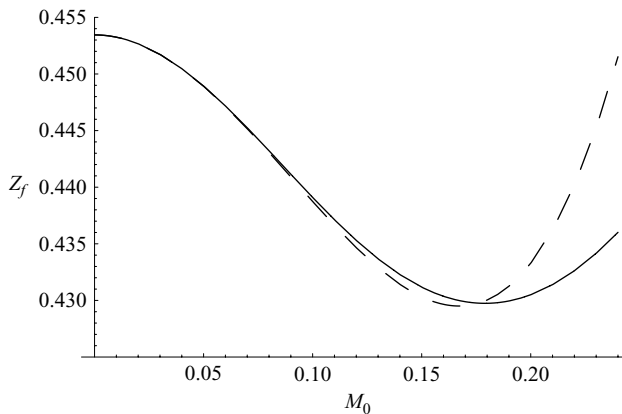


FIGURE 16. Dimensionless maximum rise height of plume, as a function of M_0 for small and moderate positive values of M_0 . Solid line: numerical integration of (4.2); dashed line: asymptotic formula (A 30) up to $O(M_0^{7/2})$.

Similar comments apply here as to the case of small negative M_0 , except that the local contribution from close to the source now consists of terms at orders M_0^2 and $M_0^{2+3n/2}$, ($n = 1, 2, \dots$). The height of zero buoyancy is reduced as a result of increased entrainment in two ways: by a global contribution (i.e. over the whole plume up to $Z = Z_n$) at $O(M_0^3)$, but more strongly (at $O(M_0^2)$) by a contribution from close to the infinite-temperature virtual source (as distinct from the finite-temperature source that applies in the case of negative M_0). This $O(M_0^2)$ reduction also applies to the maximum rise height Z_f , but is overcome at larger values of M_0 by the $O(M_0^{7/2})$ term: figure 16 shows that the local minimum value of Z_f is well predicted by the asymptotic formula up to $O(M_0^{7/2})$.

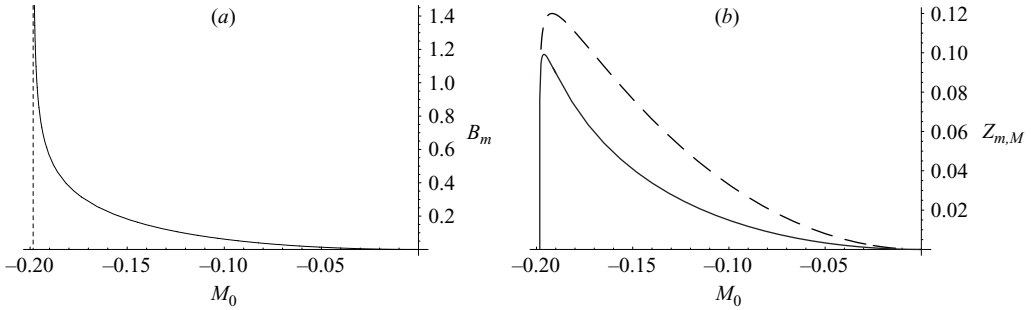


FIGURE 17. (a) Minimum half-width, and (b) heights at which minimum half-width (solid line) and maximum velocity (dashed line) are attained, as functions of M_0 for lazy rising plumes. The vertical dashed line in (a) indicates the critical value of M_0 .

(d) Large positive M_0 . As $M_0 \rightarrow \infty$:

$$Z_n \sim \frac{1}{32} M_0^{-1} - \frac{7}{2^{13} 15} M_0^{-4} + O(M_0^{-7}), \tag{A 31}$$

$$Q_f \sim M_0 + \frac{1}{8} + \frac{1}{64} M_0^{-1} + \frac{1}{768} M_0^{-2} + O(M_0^{-4}), \tag{A 32}$$

$$Z_f \sim 2^{-1/3} C_1 M_0 + \frac{\pi}{12\sqrt{3}} + \frac{3}{128} M_0^{-1} + \frac{5C_1}{2^{28/3} 3} M_0^{-2} + O(M_0^{-3}). \tag{A 33}$$

The integrals in this case only have a global contribution. The integrand decreases with increasing M_0 , reflecting the role of entrainment in decreasing the distance travelled for a given temperature decrease; hence the $O(M_0^{-1})$ behaviour of Z_n . However, the upper limit of integration for Z_f is Q_f which increases with M_0 (more cooling being required to remove a greater momentum flux), so that Z_f increases with M_0 .

A.3 Lazy rising plumes: minimum width and maximum velocity

Setting $dB/dZ=0$ and using equations (3.18), (3.20) and (3.22), we find that lazy rising plumes have their minimum half-width

$$B_m = 2Q_m^2 (8|M_0|^3 - Q_m^2)^{-1/3}, \tag{A 34}$$

where the volume flux takes the value Q_m given by

$$Q_m^2 - 2Q_m^3 = 4|M_0|^3. \tag{A 35}$$

The minimum half-width is plotted as a function of M_0 in figure 17(a).

Setting $dW/dZ=0$, noting that $W=M/Q$ and using equations (3.17), (3.18) and (3.20), lazy rising plumes are found to attain their maximum velocity

$$W_M = \left\{ \left(\frac{|M_0|}{2^{-7/3}} \right)^{-3/2} - 1 \right\}^{1/3}, \tag{A 36}$$

where the volume flux takes the value

$$Q_M = (2|M_0|)^{3/2}; \tag{A 37}$$

(A 36) has been written in a form that emphasizes the role of the critical value of M_0 , i.e. $-2^{-7/3}$. The heights Z_m and Z_M at which minimum width and maximum velocity occur can be found from integrals similar to (4.1), with Q_m and Q_M , respectively, inserted as upper limits of integration; these heights are plotted as functions of M_0

in figure 17(b). From the above formulae we obtain that $Q_m < Q_M < 1/4$ whenever $-2^{-7/3} < M_0 < 0$; since vertical distance is a smoothly increasing function of volume flux, we then have that $Z_m < Z_M < Z_n$.

Figure 17 and equation (A 36) show the singular behaviour in the limit as $M_0 \nearrow 0$: from the virtual source, an infinitesimally lazy plume contracts from infinite to infinitesimal width and accelerates from zero to unboundedly large velocity in infinitesimal distance. This reflects the unphysicality of the virtual source. The behaviour as $M_0 \rightarrow -2^{-7/3}$ is possibly easier to understand: in this limit the plume only exists within an infinitesimal range of Q values around $1/4$, so Q_m and Q_M both approach $1/4$; $B_m \rightarrow \infty$ since the plume has infinite width at its source; and the heights Z_m and Z_M both approach zero. However, a small deviation from the critical value of M_0 leads to a large decrease in minimum half-width and large increases in Z_m and Z_M . It is notable from figure 17(b) that both Z_m and Z_M increase with increasing laziness (decreasing M_0) until very close to the critical value $-2^{-7/3} \approx -0.1984$: the maximum of Z_m is when $M_0 \approx -0.1961$, while the maximum of Z_M is when $M_0 \approx -0.1919$.

Asymptotic formulae for volume flux, height and half-width at the point of minimum width are as follows.

(a) *Small negative M_0 .* As $M_0 \nearrow 0$:

$$Q_m \sim 2|M_0|^{3/2} + 4|M_0|^3 + 20|M_0|^{9/2} + O(|M_0|^6), \tag{A 38}$$

$$Z_m \sim 2^{1/3}|M_0|^2 + C_3 |M_0|^{7/2} + \frac{2^{16/3} 41}{45} |M_0|^5 + O(|M_0|^{13/2}) \tag{A 39}$$

$$\text{where } C_3 = \frac{2^{10/3} 5}{21} + \frac{2^{11/2}}{7\sqrt{3}} \int_1^{3/2} t^{-1/2}(t-1)^{-1/3} dt \approx 5.638,$$

$$B_m \sim 2^{7/3} \left(|M_0|^2 + \frac{16}{3} |M_0|^{7/2} + \frac{368}{9} |M_0|^5 + O(|M_0|^{13/2}) \right). \tag{A 40}$$

Terms at $O(|M_0|^{7/2})$ and above in (A 39) include both global and local contributions, the latter arising from terms at $O(|M_0|^3)$ and above in the upper limit of integration Q_m .

(b) *M_0 close to critical.* As $M_0 \searrow -2^{-7/3}$, in terms of the variable M_d defined in (A 19):

$$Q_m \sim \frac{1}{4} - 2^{1/3} 3M_d + 2^{14/3} 3M_d^2 - 3200M_d^3 + O(M_d^4), \tag{A 41}$$

$$Z_m \sim 3^{2/3} \left(2^{-41/18} C_1 M_d^{1/6} - \frac{2^{-19/9} 13}{3} M_d^{2/3} - \frac{2^{1/18} 5}{21} C_1 M_d^{7/6} + \frac{2^{20/9} 21}{5} M_d^{5/3} + O(M_d^{13/6}) \right), \tag{A 42}$$

$$B_m \sim 3^{-1/3} \left(2^{-22/9} M_d^{-1/3} - \frac{2^{26/9}}{3} M_d^{2/3} + \frac{2^{29/9} 23}{9} M_d^{5/3} + O(M_d^{8/3}) \right). \tag{A 43}$$

where C_1 is defined in (A 17). Terms at $O(M_d^{2/3})$ and $O(M_d^{2/3+n})$ ($n = 1, 2, \dots$) include local contributions arising from terms at $O(M_d)$ and above in the upper limit of integration Q_m , with considerably larger coefficients than the global contributions at the respective orders. In particular, the term $-2^{1/3} 3M_d$ in the expansion for Q_m gives rise to a corresponding negative local contribution to Z_m at $O(M_d^{2/3})$, 12 times greater than the global contribution at that order; it is this local contribution which

is responsible for the maximum in Z_m occurring at such a small value of M_d (i.e. with M_0 close to $-2^{-7/3}$).

A.4 Strongly forced descending plumes: minimum velocity

Similarly to the case of maximum velocity for lazy rising plumes (§A.3 above), we find that the minimum velocity

$$W_m = \left\{ 1 - \left(\frac{M_0}{2^{-7/3}} \right)^{-3/2} \right\}^{1/3} \tag{A 44}$$

for descending plumes occurs where the volume flux takes the value

$$Q_M = (2M_0)^{3/2}. \tag{A 45}$$

Since $Q_M > 1/4$ for $M_0 > 2^{-7/3}$, the minimum of velocity occurs at a greater depth below the source than the point of zero buoyancy.

For near-critical forcing, we use the notation

$$M_D = M_0 - 2^{-7/3}. \tag{A 46}$$

The case of forcing just above critical is important because of the effect of low velocities on the distance travelled by a plume: as $M_0 \searrow 2^{-7/3}$,

$$W_m \sim 3^{1/3} 2^{4/9} M_D^{1/3} + O(M_D^{4/3}), \tag{A 47}$$

with the $1/3$ power of M_D indicating a sharp rise in W_m as M_0 increases from the critical value.

A.5 Descending plumes: far-field asymptotics

For strongly forced plumes and all cool plumes,

$$M \sim \left(Q - \frac{1}{8} - \frac{1}{64} Q^{-1} + \left(\frac{M_0^3}{3} - \frac{5}{1536} \right) Q^{-2} + O(Q^{-3}) \right) \quad \text{as } Q \rightarrow \infty. \tag{A 48}$$

As $Z \rightarrow \infty$,

$$Q \sim Z - \frac{1}{8} \ln Z + O(1), \tag{A 49}$$

$$M \sim Z - \frac{1}{8} \ln Z + O(1), \tag{A 50}$$

$$B \sim Z - \frac{1}{8} \ln Z + O(1), \tag{A 51}$$

$$W \sim 1 - \frac{1}{8} Z^{-1} - \frac{1}{64} Z^{-2} \ln Z + O(Z^{-2}). \tag{A 52}$$

The $O(1)$ terms in (A 49)–(A 51) and the $O(Z^{-2})$ term in (A 52) arise from a region within distance $Z \sim O(1)$ from the source, and are dependent on the source condition, i.e. the value of M_0 . Thus plumes with different degrees of forcing or laziness at their source will differ in their volume flux, momentum flux and half-width by constant amounts in the far field.

A.6 Strongly forced descending plumes: depth of zero buoyancy

The notations (A 46), (A 17) and (A 18) are used in the formulae below, which are again obtained using the methods described in §A.2.

(a) M_0 above, but close to, critical. As $M_0 \searrow 2^{-7/3}$:

$$Z_n \sim 2^{-8/3}(C_2 + 1) - 2^{-41/18} 3^{7/6} C_1 M_D^{1/6} + 2^{-19/9} 3^{-1/3} M_D^{2/3} + \frac{2^{-1/3} 3}{5} M_D - \frac{2^{1/18} 3^{1/6} 5}{7} C_1 M_D^{7/6} + O(M_D^{5/3}). \quad (\text{A } 53)$$

The leading-order (constant) term and terms of order M_D^n ($n=1, 2, \dots$) are global contributions, while the terms at orders $M_D^{1/6}$ and $M_D^{(1+3n)/6}$ ($n=1, 2, \dots$) are local contributions from the region where $1/4 - Q = O(M_D^{1/2})$ at the end of the integration range; the latter terms are similar to the expansion (A 21) for Z_n for rising plumes with near-critical forcing (in which all terms are local, since the length of the integration range approaches zero as $M_0 \rightarrow -2^{-7/3}$). These local contributions relate to the distance travelled at low velocity close to the zero-buoyancy point for near-critically forced plumes.

(b) Large positive M_0 . As $M_0 \rightarrow \infty$:

$$Z_n \sim \frac{1}{32} M_0^{-1} + \frac{7}{2^{13} 15} M_0^{-4} + O(M_0^{-7}). \quad (\text{A } 54)$$

Note the similarity to the formula (A 31) for rising plumes; the same comments apply as in §A.2(d).

A.7 Warm weakly forced descending plumes: total distance travelled

We again use the notations (A 46), (A 17) and (A 18).

(a) Small M_0 . As $M_0 \searrow 0$:

$$Z_f \sim 2M_0^2 + \frac{2^{11/2} 3^{1/2} C_1}{7} M_0^{7/2} + O(M_0^5). \quad (\text{A } 55)$$

The upper limit of integration in (4.2) is $O(M_0^{3/2})$ (as given by (A 24)), and the integrand is $O(M_0^{1/2})$.

(b) M_0 below, but close to, critical. As $M_0 \nearrow 2^{-7/3}$:

$$Z_f \sim 2^{-8/3}(C_2 + 1) - 2^{-23/18} 3^{2/3} C_1 |M_D|^{1/6} - \frac{2^{-1/3} 3}{5} |M_D| + \frac{2^{19/18} 5 C_1}{3^{1/3} 7} |M_D|^{7/6} + O(|M_D|^2) \quad (\text{A } 56)$$

Note the similarities to the expansion (A 53) for plumes just on the strong side of critical forcing. The analysis in terms of global and local contributions is similar to that case, except that the upper limit of integration here is Q_f rather than $1/4$ (but with Q_f close to $1/4$ as given by (A 20)).

A.8 Descending plumes: minimum width

Equations (5.1) and (5.2) give the volume flux Q_m and plume half-width B_m at the neck, and the distance from the virtual source to the neck is

$$Z_m = \int_{Q_0}^{Q_m} \frac{Q}{M} dQ. \quad (\text{A } 57)$$

(a) Large negative M_0 . As $M_0 \rightarrow -\infty$:

$$Q_m \sim 2^{1/3} |M_0| + \frac{1}{6} + \frac{2^{-7/3}}{9} |M_0|^{-1} + \frac{2^{-8/3}}{81} |M_0|^{-2} + O(|M_0|^{-4}), \quad (\text{A } 58)$$

$$Z_m \sim 2^{-4/3}(2 - C_1)|M_0| + \frac{1}{24}(2^{1/3} + C_4(2)) + \frac{19}{1152}|M_0|^{-1} + O(|M_0|^{-2}), \quad (\text{A } 59)$$

$$B_m \sim 2^{2/3}|M_0| + 2^{-5/3} + \frac{1}{24}|M_0|^{-1} + O(|M_0|^{-2}), \quad (\text{A } 60)$$

where C_1 is given by (A 17) and

$$C_4(k) = \int_1^k t^{-2/3}(t-1)^{-1/3} dt \quad (\text{A } 61)$$

with $C_4(2) \approx 1.2290$. There are local contributions to the integral for Z_m at $O(1)$ and higher orders due to the terms in the upper limit of integration Q_m at these orders.

(b) *Small (positive or negative) M_0 .* As $M_0 \rightarrow 0$:

$$Q_m \sim \frac{1}{2} - 8M_0^3 - 256M_0^6 + O(M_0^9) \quad (\text{A } 62)$$

$$Z_m \sim \left(2^{-7/3} + \frac{1}{8}C_4\left(\frac{4}{3}\right)\right) + \frac{2^{20/3}23}{15}M_0^6 + O(M_0^9), \quad (\text{A } 63)$$

$$B_m \sim 2^{-1/3} - \frac{2^{14/3}}{3}M_0^3 - \frac{2^{26/3}5}{9}M_0^6 + O(M_0^9), \quad (\text{A } 64)$$

with $C_4(4/3) \approx 0.6662$. At $O(M_0^3)$ in the integral for Z_m there is exact cancellation between global and local contributions: as M_0 increases above zero, the plume temperatures at the source and the neck move towards the temperature of zero buoyancy; thus buoyancy forces are smaller throughout its trajectory from source to neck, leading to smaller velocity, less entrainment, and hence an increase in Z_m with M_0 in the global contribution; but this is balanced by a decrease in Z_m in the local contribution from the upper limit of integration, due to the neck occurring at a lower value of volume flux when M_0 is greater.

(c) *Critically forced plumes.* For $M_0 = M_c$:

$$Q_m = \frac{1 + \sqrt{5}}{8} \approx 0.4045, \quad (\text{A } 65)$$

$$Z_m = 2^{-13/3}(\sqrt{5} + 1)^{5/3} + \frac{1}{8} \int_0^{(\sqrt{5}-1)/3} t^{-2/3}(1+t)^{-1/3} dt \approx 0.6219, \quad (\text{A } 66)$$

$$B_m = 2^{-10/3}(\sqrt{5} + 1)^{5/3} \approx 0.7024. \quad (\text{A } 67)$$

(d) *Strongly forced plumes.* The above Z_m -values are measured from finite-temperature sources, so there is no meaningful comparison with distances from the infinite-temperature sources for strongly forced plumes. However, the volume flux and width at the neck vary smoothly through the critical value $M_0 = 2^{-7/3}$. At $M_0 = 2^{-2/3}/3$, the greatest value of M_0 for which a neck exists, we find $Q_m = 1/3$ and $B_m = 2/3$, which are the minimum values of volume flux and half-width at a neck for any descending plumes.

REFERENCES

- BATCHELOR, G. K. 1967 *An Introduction to Fluid Dynamics*. Cambridge University Press.
 BLOOMFIELD, L. J. & KERR, R. C. 1998 Turbulent fountains in a stratified fluid. *J. Fluid Mech.* **358**, 335–356.
 BLOOMFIELD, L. J. & KERR, R. C. 2000 A theoretical model of a turbulent fountain. *J. Fluid Mech.* **424**, 197–216.

- CAULFIELD, C.-C. P. & WOODS, A. W. 1995 Plumes with non-monotonic mixing behaviour. *Geophys. Astrophys. Fluid Dyn.* **79**, 173–199.
- FISCHER, H. B., LIST, E. J., KOH, R. C. Y., IMBERGER, J. & BROOKS, N. H. 1979 *Mixing in Inland and Coastal Waters*. Academic.
- FOSTER, T. D. 1972 An analysis of the cabbelling instability in sea water. *J. Phys. Oceanogr.* **2**, 294–301.
- GU, R. & STEFAN, H. G. 1988 Analysis of turbulent buoyant jet in density-stratified water. *J. Environ. Engng ASCE* **114**, 878–897.
- GU, R. & STEFAN, H. G. 1993 Submerged warm water jet discharge in an ice-covered reservoir or lake. *Cold Regions Sci. Technol.* **21**, 151–168.
- HINCH, E. J. 1991 *Perturbation Methods*. Cambridge University Press.
- HOGLUND, B. & SPIGARELLI, S. A. 1972 Studies of the sinking plume phenomenon. In *Proc. 15th Conf. Great Lakes Res.*, pp. 614–624. International Association of Great Lakes Research.
- HUNT, G. R. & KAYE, N. B. 2005 Lazy plumes. *J. Fluid Mech.* **533**, 329–338.
- LEE, S.-L. & EMMONS, H. W. 1961 A study of natural convection above a line fire. *J. Fluid Mech.* **11**, 353–368.
- MACQUEEN, J. F. 1979 Turbulence and cooling water discharges from power stations. In *Mathematical Modelling of Turbulent Diffusion in the Environment* (ed. C. J. Harris), pp. 379–437.
- MARMOUSH, Y. R., SMITH, A. A. & HAMBLIN, P. F. 1984 Pilot experiments on thermal bar in lock exchange flow. *J. Energy Engng* **110**, 215–227.
- MOORE, D. R. & WEISS, N. O. 1973 Nonlinear penetrative convection. *J. Fluid Mech.* **61**, 553–581.
- MORTON, B. R. 1959 Forced plumes. *J. Fluid Mech.* **5**, 151–163.
- MORTON, B. R., TAYLOR, G. I. & TURNER, J. S. 1956 Turbulent gravitational convection from maintained and instantaneous sources. *Proc. R. Soc. Lond. A* **234**, 1–23.
- OOSTHUIZEN, P. H. AND PAUL, J. T. 1996 A numerical study of the steady state freezing of water in an open rectangular cavity. *Intl J. Numer. Meth. Heat Fluid Flow* **6**, 3–16.
- ROUSE, H., YIH, C. S., & HUMPHREYS, H. W. 1952 Gravitational convection from a boundary source. *Tellus* **4**, 201–210.
- TURNER, J. S. 1962 The ‘starting plume’ in neutral surroundings. *J. Fluid Mech.* **13**, 356–368.
- TURNER, J. S. 1966 Jets and plumes with negative and reversing buoyancy. *J. Fluid Mech.* **26**, 779–792.
- TURNER, J. S. 1973 *Buoyancy Effects in Fluids*. Cambridge University Press.
- TURNER, J. S. 1986 Turbulent entrainment: The development of the entrainment assumption, and its application to geophysical flows. *J. Fluid Mech.* **173**, 431–471.
- TURNER, J. S. & CAMPBELL, I. H. 1987 Temperature, density and buoyancy fluxes in ‘black smoker’ plumes, and the criterion for buoyancy reversal. *Earth Planet. Sci. Lett.* **86**, 85–92.
- WÜEST, A., BROOKS, N. H. & IMBODEN, D. M. 1992 Bubble plume modeling for lake restoration. *Water Resources Res.* **28**, 3235–3250.